TOPICAL REVIEW

Particle acceleration and relativistic shocks

J.G. Kirk† and P. Duffy‡

† Max-Planck-Institut für Kernphysik, Postfach 10 39 80, D–69029 Heidelberg, Germany

‡ Department of Mathematical Physics, University College Dublin, Belfield, Dublin 4, Ireland

Abstract.

Observations of both gamma-ray burst sources and certain classes of active galaxy indicate the presence of relativistic shock waves and require the production of high energy particles to explain their emission. In this paper we first review the basic theory of shock waves in relativistic hydrodynamics and magneto-hydrodynamics, emphasising the astrophysically interesting cases. This is followed by an overview of the theory of particle acceleration at such shocks. Whereas, for diffusive acceleration at non-relativistic shocks, it is the compression ratio which fixes the energetic particle spectrum uniquely, acceleration at relativistic shocks is more complicated. In the absence of scattering, particles are simply 'compressed' as they pass through the shock front. This mechanism – called shock-drift acceleration – enhances the energy density in accelerated particles, but does so without changing the spectral index of upstream particles. Scattering due to MHD waves leads to multiple encounters between the particles and the shock front, producing an energetic particle population which depends on the properties of the shock front and the level and nature of particle scattering. We describe the method of matching the angular distributions of the upstream and downstream distributions at the shock front which leads to predictions of the spectral index. Numerical simulation of particle transport provides an alternative means of calculating spectral indices, and has recently been extended to cover ultra relativistic shocks. We review these calculations and summarise the applications to the astrophysics of relativistic jets and fireball models of gamma-ray-bursts.

PACS numbers: 00.00, 20.00, 42.10

1. Introduction

Within the space of thirty minutes, the power emitted in very high energy gamma-rays by an active galaxy at a distance of several hundred million light years has been observed to increase more than twenty fold [1]. This unexpected observation has raised new questions concerning the nature of 'gamma-ray blazars', as this class of source is called. In a parallel development, the discovery that at least some of the enigmatic, powerful so-called 'gamma-ray burst' sources lie at cosmological distances [2] was perhaps less surprising to many astrophysicists, but nonetheless places stringent restrictions on the conditions prevalent in the emission regions. These two recent developments have been responsible for a renewed focusing of attention on the subject of relativistic shock fronts. In each case, the observations imply that the photon density in the source is so large, that the gamma-rays would be subject to strong absorption due to photon-photon interactions, were not the source moving in our direction with a speed close to that of light. The implied Lorentz factors are about 50-100 in the case of the active galaxies, and several hundreds in the case of gamma-ray burst sources.

The subject is not new. Relativistic motion was proposed as a way out of the rapid variability problem over thirty years ago [3]. The observational motivation then was similar to that of today: in order for the variable synchrotron emission in the radio band observed from active galaxies to emerge without being subject to self-absorption an improbably weak magnetic field was implied. The proposed solution was that the source moves at relativistic speed towards the observer, a Lorentz factor of 5–10 being sufficient to remove the difficulty. The hypothesis was impressively confirmed by sequences of radio observations of the cores of active galaxies, using very long baseline radio interferometry, which clearly showed rapid expansion. This apparently 'superluminal' motion is now seen in many sources, and indicates the outflow of plasma containing relativistic electrons and magnetic fields with bulk Lorentz factors between roughly 5 and 20 [4].

Shock fronts are an inevitable consequence when such flows encounter the ambient material in the interstellar medium of the host galaxy, or in the intergalactic medium. Indeed, they seem the natural sites for the dissipation of the kinetic energy associated with the relativistic motion itself. Furthermore, wherever we directly observe shock fronts in astrophysics – from the Earth's bow shock to supernova remnants – they are associated with particle acceleration. The radiation from both gamma-ray bursts and gamma-ray blazars requires the presence of particles (most likely electrons and/or positrons) with very high Lorentz factors (exceeding 10^6 in blazars), so that particle acceleration must be happening there too. The aim of this review is to summarise our current theoretical picture of relativistic shocks in astrophysics and, in particular, our ideas about the way in which they might accelerate particles. Section 2 presents an overview of hydrodynamic and MHD shocks, Section 3 examines shock drift acceleration as well as analytic and numerical methods of treating Fermi acceleration and Section 4 briefly summarises the applications to relativistic jets and gamma-ray bursts.

2. Relativistic Shocks

Relativistic effects can be important at shock fronts for two distinct reasons. Firstly, the post shock temperature can be so high that the thermal motion of individual particles approaches the speed of light. Secondly, it is possible that so much energy is released into a region containing relatively little matter that the subsequent expansion proceeds at a bulk speed approaching that of light. It is certainly possible for the former effect to arise when all bulk velocities are quite modest. For example, a hot plasma in which the pressure is provided predominantly by photons is always relativistic in this sense, and behaves as a gas whose ratio of specific heats is $4/3$. If the mass density in such a plasma is dominated by atoms or ions, there exists a sound velocity which is determined by the pressure of the photons and the inertia of the ions and which can be small compared to the speed of light. Downstream of a strong shock front in such a plasma, the bulk speed is, of course, less than this sound speed, whereas the upstream fluid speed (provided it is still non-relativistic) is equal to seven times the downstream speed. On the other hand, it seems unlikely that in a realistic situation a relativistic bulk flow could be thermalised by a shock front without producing thermal velocities which are also relativistic. As a consequence, the fully relativistic equation of state of a plasma should be used to investigate the possible jump conditions.

Following the solution of the relativistic shock problem in hydrodynamics by Taub [5], the question of which types of shock discontinuities are permitted and what the jump conditions are in the ideal MHD picture was investigated by de Hoffmann & Teller [6]. The full relativistic theory was presented by Akhiezer & Polovin [7] and an elegant summary of the most important results has been given by Lichnerowicz [8]. However, the generality of these treatments makes them less accessible to the plasma astrophysics community, and several papers have worked out special cases, sometimes using particular approximations to the equation of state [9, 10, 11].

In view of this, we present in this Section the basic, astrophysically relevant, results on both hydrodynamic and MHD shocks in as simple a form as is compatible with completeness. In each case a numerical treatment is in general needed to solve for the jump conditions, and we provide in the Appendices a detailed description of how such an algorithm can be constructed. In the case of hydrodynamic shocks, the approximate formulae for strong shocks and for the ultra-relativistic case are presented, their derivations being relegated to the Appendix. The special cases which are of most interest in MHD are those of weak magnetic field and of ultra relativistic, perpendicular shocks. Again, the relevant results are quoted and the derivations presented in the Appendix. We also note that ultra-relativistic switch-on shocks are possible only in a very limited parameter range.

The most important property of a shock front for the acceleration problem is its compression ratio, and it has been known for some time [12] that increasing the magnetic field strength tends to reduce the compression. We present some figures at the end of the section which illustrate this effect.

2.1. Hydrodynamics

It is useful at this point to recall the theory of relativistic hydrodynamics and the shock wave solutions it admits. This will also serve as a means of introducing the notation we will use throughout this paper.

In the absence of external forces and energy sources, the equations of relativistic hydrodynamics can be formulated as the vanishing divergence of the stress-energy tensor associated with the fluid:

$$\nabla_\mu T^{\mu\nu} = 0 \tag{1}$$

(e.g., [13]). Neglecting dissipative effects, the stress-energy tensor is diagonal in the local plasma rest frame, and is given by

$$T^{\mu\nu} = w u^\mu u^\nu + p g^{\mu\nu} \tag{2}$$

Here u^μ is the four velocity of the fluid ($\mu = 0, 1, 2, 3$), and $g^{\mu\nu}$ the metric tensor, for which we adopt the convention $-{+}{+}{+}$. The scalars w and p are the proper enthalpy density and pressure, i.e., those measured in the rest frame of the fluid, in which $u^\mu = (1, 0, 0, 0)$.

The problem of solving the Rankine-Hugoniot relations to find the jump conditions across a shock front requires one to use an equation of state to find the quantity p/ρ, given the quantity e/ρ. For a dissipation free ideal gas, the Synge equation described in Appendix A is appropriate, and it is necessary to solve Eq. (A9) numerically. Although this procedure is straightforward, a popular short-cut is to define a parameter $\hat{\gamma}$ via the equation

$$p = (\hat{\gamma} - 1)(e - \rho) \tag{3}$$

[14, 15], which replaces the equation of state (A9). In the non-relativistic case $\hat{\gamma} = 5/3$ and can be identified as the ratio of specific heats of the gas. For a gas whose pressure is dominated by a relativistic component, one has $\hat{\gamma} = 4/3$ (a fully relativistic gas has, in addition, $e \gg \rho$). For a gas consisting of equal numbers of electrons and protons in thermodynamic equilibrium with each other, there is a range of temperatures $m_\mathrm{p} \gg T \gg m_\mathrm{e}$ in which $\hat{\gamma} \approx 13/9$ (here m_e is the electron mass and m_p the proton mass).

The jump conditions across a relativistic hydrodynamic shock are given by Eq. (1), which expresses the laws of energy and momentum conservation, together with the law of conservation of particle number. For those constituents which are neither created nor annihilated in the shock, one has

$$\nabla_\mu(n_i u^\mu) = 0 \tag{4}$$

The shock wave is a surface in space-time, $\phi(x_\mu) = 0$, across which there is a discontinuity in the fluid variables. The shock normal is given by $l_\mu = \partial_\mu \phi$ and, without loss of generality, we normalise ϕ so that $l^\mu l_\mu = 1$. Two frames of reference which are important from a physical point of view are those in which the upstream and downstream plasma is at rest. Defining the Lorentz scalars v_- and v_+ to be the shock speed measured in the upstream and downstream rest frames respectively, one has

$$v_\pm = \frac{|u^\mu_\pm l_\mu|}{\sqrt{1+|u^\mu_\pm l_\mu|^2}}. \tag{5}$$

where u^μ_- and u^μ_+ are the 4-velocities of the plasma immediately upstream and immediately downstream of the shock front, respectively.

Whenever necessary, we will use Cartesian coordinates in which the shock normal is along the x-axis. In the upstream and downstream rest frames $l_\mu = (\Gamma_\pm v_\pm, \Gamma_\pm, 0, 0)$, where $\Gamma_\pm = (1 - v^2_\pm)^{-1/2}$. As we show below, for a hydrodynamic shock front, the downstream plasma flows along the shock normal, as seen from the upstream rest frame, so that in this frame $u^\mu_+ = (\Gamma_{\rm rel}, -\Gamma_{\rm rel} v_{\rm rel}, 0, 0)$, where

$$v_{\rm rel} = \frac{v_- - v_+}{1 - v_- v_+} \tag{6}$$

is the relative speed of the upstream gas with respect to the downstream gas, and its related Lorentz factor is $\Gamma_{\rm rel}$.

From the conservation laws, the shock jump conditions are

$$[n_i u^\mu]\, l_\mu = 0 \tag{7}$$

$$[T^{\mu\nu}]\, l_\mu = 0. \tag{8}$$

where (7) is valid for all conserved constituents. For non-conserved particles additional information is required specifying the number density, for example via the equation of state. In the shock rest frame, with the shock normal and upstream flow velocity along the x-axis it is straightforward to show that the downstream flow velocity is also directed along the same axis. In this frame equations (7) and (8) can be written as

$$\Gamma_- \rho_- v_- = \Gamma_+ \rho_+ v_+ \tag{9}$$

$$\Gamma^2_- w_- v^2_- + p_- = \Gamma^2_+ w_+ v^2_+ + p_+ \tag{10}$$

$$\Gamma^2_- w_- v_- = \Gamma^2_+ w_+ v_+ \tag{11}$$

Given v_- and the upstream state, e_-/ρ_-, these equations are to be solved for the downstream state v_+, e_+/ρ_- and the proper compression ratio $R \equiv \rho_+/\rho_-$. In general, this entails a numerical procedure, which is described in Appendix A. However, there are several interesting special cases with analytic solutions:

(i) In the limit of non-relativistic fluid speeds, $v_\pm \ll 1$, the well-known Rankine-Hugoniot conditions are recovered. In terms of the upstream Mach number

$$M_- = v_- \left(\frac{\hat{\gamma} p_-}{\rho_-}\right)^{-1/2} \tag{12}$$

one has

$$\begin{aligned} p_+ &= \rho_- v_-^2 \left[\frac{2}{(\hat{\gamma}+1)} - \frac{(\hat{\gamma}-1)}{\hat{\gamma}(\hat{\gamma}+1)M_-^2}\right] \\ v_+ &= v_- \left[\frac{(\hat{\gamma}-1)}{(\hat{\gamma}+1)} + \frac{2}{(\hat{\gamma}+1)M_-^2}\right] \\ \frac{\rho_+}{\rho_-} &= \frac{\hat{\gamma}+1}{\hat{\gamma}-1+(2/M_-^2)} \end{aligned} \tag{13}$$

where in our case of a monatomic gas, the relevant value of the adiabatic index is $\hat{\gamma} = 5/3$.

(ii) For a shock in a relativistic gas, in which $p = e/3$ (both upstream and downstream) one finds the simple relation

$$v_- v_+ = \frac{1}{3} \tag{14}$$

However, this corresponds to the perhaps less interesting case of a relativistic shock moving into unshocked gas in which the total energy density significantly exceeds that corresponding to rest-mass i.e., $e_- \gg \rho_-$.

(iii) For a strong shock, at which the upstream pressure can be neglected, the equation of state in the upstream gas is unimportant. Furthermore, if particles are conserved at the shock, the average Lorentz factor of a particle does not change across the shock as seen from the downstream rest frame, i.e., $e_+ = \Gamma_{\rm rel}\rho_+$ (see Appendix A, (Eq. A20) with $\eta = 1$). Then, using, for the downstream medium, the equation of state for fixed adiabatic index (Eq. 3) one may derive

$$\begin{aligned} w_+/\rho_+ &= \hat{\gamma}(\Gamma_{\rm rel}-1)+1 \\ \Gamma_-^2 &= \frac{(w_+/\rho_+)^2(\Gamma_{\rm rel}+1)}{\hat{\gamma}(2-\hat{\gamma})(\Gamma_{\rm rel}-1)+2} \end{aligned} \tag{15}$$

[14], which gives the shock speed and downstream pressure in terms of the relative velocity of the upstream and downstream fluids. These relations are generalised in Appendix A to the case in which particles are created at the shock front.

(iv) In the ultra-relativistic limit, $\Gamma_- \to \infty$, the upstream pressure (p_-) may be neglected in Eq. (10). If, in addition, the downstream particles are ultra-relativistic, in the sense that $e_+ \gg \rho_+$, one may combine Eqs. (10), (11) and (6) to find:

$$v_+ \to \hat{\gamma} - 1 = 1/3 \tag{16}$$
$$\Gamma_{\rm rel} \to \Gamma_- \sqrt{(2-\hat{\gamma})/\hat{\gamma}} = \Gamma_-/\sqrt{2} \tag{17}$$

These relations are independent of the equations of state upstream and downstream and hold whether or not particles are conserved at the shock, provided only that the downstream particles are ultra-relativistic.

2.2. Magnetohydrodynamic Shocks

In ideal, relativistic MHD, it is assumed that the plasma is dissipation free and that in the local rest frame the electric field vanishes. In this case, the electromagnetic field is specified by the magnetic field alone, and the system is described by the four 'source-free' equations of Maxwell: $\nabla_\mu(*F^{\mu\nu}) = 0$ where $*F_{\mu\nu}$ is the dual electromagnetic field tensor,

$$*F_{\mu\nu} = \begin{pmatrix} 0 & B_1 & B_2 & B_3 \\ -B_1 & 0 & E_3 & -E_2 \\ -B_2 & -E_3 & 0 & E_1 \\ -B_3 & E_2 & -E_1 & 0 \end{pmatrix} \tag{18}$$

where $\mathbf{B} = (B_1, B_2, B_3)$ and $\mathbf{E}$ are the magnetic and electric fields as measured in a frame where the plasma's three velocity is $\vec{\beta}$, augmented by the generalised (ideal) Ohm's Law $\mathbf{E} = -\vec{\beta} \times \mathbf{B}$, which constrains the electric field to vanish in the plasma rest frame. Defining the four-vector $B_\mu = -u^\nu(*F_{\mu\nu})$ the field tensor can be written as $*F^{\mu\nu} = B^\mu u^\nu - u^\mu B^\nu$ so that the source-free Maxwell equations become

$$\nabla_\mu \left(B^\mu u^\nu - u^\mu B^\nu\right) = 0. \tag{19}$$

In the rest frame of the plasma $B^\mu = (0, \mathbf{B})$ where $\mathbf{B}$ is the magnetic field three vector in that frame. In the following, B is taken to denote the magnetic field strength in the local plasma rest frame which satisfies $B^\mu B_\mu = B^2$. The components of B^μ in a frame where the plasma is moving with four velocity u^μ can be derived from the appropriate Lorentz transformation in terms of $\mathbf{B}$. The energy momentum tensor of the system consisting of electromagnetic fields and fluid is

$$T^{\mu\nu} = \left(w + \frac{B^2}{4\pi}\right) u^\mu u^\nu + \left(p + \frac{B^2}{8\pi}\right) g^{\mu\nu} - \frac{B^\mu B^\nu}{4\pi}. \tag{20}$$

and the equations of relativistic MHD consist of the vanishing divergence of this tensor, together with (19) and, of course, an equation of state for the fluid. An important difference between relativistic and non-relativistic MHD is that in relativistic MHD it is not possible simplify (19) by ignoring the displacement current. This is because in the relativistic case, fluctuations in the space charge cannot be neutralised on a time scale which is much faster than the other dynamical time-scales.

There are three wave modes in MHD, the fast and slow magnetosonic modes, and the Alfvén mode. The phase velocities of these modes in a given direction will be denoted by $v_{\rm fast}$, $v_{\rm slow}$ and $v_{\rm A}$. Quite generally one has

$$v_{\rm fast} \geq v_{\rm A} \geq v_{\rm slow} \tag{21}$$

Defining Φ as the angle between the magnetic field and the direction of propagation, measured in the plasma rest frame, the Alfvén wave has the speed

$$v_{\rm A} = \sqrt{\frac{B^2/(4\pi)}{w + B^2/(4\pi)}} \cos\Phi \tag{22}$$

and the fast and slow mode speeds are the roots of the equation

$$w(v_{\rm s}^{-2} - 1)v^4 - \left[w + \frac{B^2}{4\pi v_{\rm s}^2}\right] v^2(1 - v^2) + \frac{B^2}{4\pi}\cos^2\Phi(1 - v^2) = 0 \tag{23}$$

[10]. These wave speeds are important for the properties of shock fronts [7, 8], since, as in the non-relativistic case [16, 17], a physically realisable shock front cannot provide a transition across the Alfvénic point in ideal MHD. In other words, the two kinds of transition available are the slow-mode shock, with

$$\begin{aligned} &v_{\rm A-} > v_- > v_{\rm slow-} \\ &v_{\rm A+} > v_{\rm slow+} > v_+ \end{aligned} \tag{24}$$

and the fast-mode shock which has

$$\begin{aligned} &v_- > v_{\rm fast-} > v_{\rm A-} \\ &v_{\rm fast+} > v_+ > v_{\rm A+} \end{aligned} \tag{25}$$

where $v_{\rm fast,A,slow\pm}$ refer to the propagation speeds along the normal to the shock front in the up and downstream regions. The fast-mode shock is associated with an increase in the magnetic field strength across the shock, whereas the slow-mode shock results in a decrease of the field.

For the purposes of numerical simulation of a relativistic MHD flow, it is interesting to put the governing equations into divergence form, avoiding the additional algebraic constraint implied by the relation $u^\mu B_\mu = 0$. Such a formulation has been presented [18] and implemented [19] by van Putten. However, at least for the non-relativistic case, other methods are available (e.g., Falle et al. [20]) and there is also no advantage to be gained by such a reformulation in the investigation of the jump conditions. These are determined by the equations of conservation of particles and of energy/momentum (7) and (8) [as in the hydrodynamic case, but with the modified stress-energy tensor of Eq. (20)], supplemented by equation (19) which implies:

$$[B^\mu u^\nu - u^\mu B^\nu]\, l_\mu = 0. \tag{26}$$

It proves convenient to define $b^\mu_\pm \equiv B^\mu_\pm/\sqrt{4\pi\rho_-}$ so that $|b|^2_\pm = B^2_\pm/4\pi\rho_-$ is *twice* the ratio of the magnetic field energy density in the local plasma rest frame to the upstream rest mass energy density. In the upstream and downstream rest frames we define $\Phi_\pm$ to be the angle between the magnetic field and the shock front's direction of propagation, and take coordinates such that the field lies in the x–z plane. Therefore we can write for the two vectors b_+ and b_-

$$b^\mu_\pm = (4\pi\rho_-)^{-1/2}(0, B_\pm \cos\Phi_\pm, 0, B_\pm \sin\Phi_\pm) \tag{27}$$

in the upstream or downstream frame as appropriate. Given v_-, Φ_- and $|b|^2_-$, the jump conditions can be solved numerically to find v_+, Φ_+, $|b|^2_+$ and the compression ratio ρ_+/ρ_- using the method of Majorana & Anile [10], which is described in Appendix B, and involves a single one-dimensional root-finding operation.

In general, the plane which contains the shock normal and the upstream magnetic field, as seen in the upstream rest frame, also contains the plasma velocity and the magnetic field in the downstream half-space – i.e., these shocks do not permit the generation of a non-coplanar magnetic field. However, in addition to the fast-mode and slow-mode shocks, there exist solutions of the jump conditions (known as rotational discontinuities), which propagate with the Alfvén speed and do not involve a compression of the plasma, or a change in the field strength, but merely a change in the direction of the field and the plasma speed. In the standard picture of Fermi acceleration, they are not expected to accelerate particles. Slow mode shocks are also thought to be ineffective accelerators. Not only does the magnitude of the magnetic field decrease across the shock, (rendering shock drift acceleration ineffective) but also, if particle scattering is produced by Alfvén waves, then the speed of the scattering centres in the fluid frame exceeds the speed of the slow mode shock. Crossing and recrossing would then lead to a net deceleration if the waves predominantly stream away from the shock front, which would turn diffusive acceleration into diffusive deceleration [21]. Therefore, only fast-mode shocks are considered in the following.

As in the hydrodynamical case, there are some interesting limiting cases for MHD shocks:

(i) In the case of a weak, dynamically unimportant magnetic field, such as considered by Kirk & Heavens [22], Begelman & Kirk [23] several useful analytic results can be obtained. Of course, the jump conditions for the plasma speed and temperature are identical to the hydrodynamical case. In the shock rest frame with both v_-

and v_+ directed along the x-axis, the x-component of magnetic field is conserved across the shock. Since the component of magnetic field in the direction of the flow velocity is unchanged by a Lorentz boost to the local fluid frame this gives a simple expression connecting the angles Φ_- and Φ_+,

$$B_- \cos\Phi_- = B_+ \cos\Phi_+ \tag{28}$$

The (proper) compression in the magnetic field can be related to the upstream parameters and the compression ratio $r = v_-/v_+ = R\Gamma_+/\Gamma_-$ of the fluid:

$$R_B \equiv \frac{B_+}{B_-} = \left[r^2 - \Gamma_-^2(r^2-1)(\cos^2\Phi_- - v_-^2)\right]^{1/2} \tag{29}$$

(ii) If the upstream plasma flows along the magnetic field and the shock normal, it is possible to have a purely hydrodynamic transition in which the downstream flow is also along the magnetic field. However, for some parameter ranges, it is also possible to generate a transverse component of the field at the shock front in what is called a 'switch-on' shock. This happens if the hydrodynamic solution violates the constraints given by (24) and (25) (referred to as evolutionarity conditions†). To find the relevant range of parameters in the ultra-relativistic case, we make the approximations

$$\begin{aligned} &v_- \to 1; \qquad v_+ \to 1/3; \qquad \Gamma_+ \to 3\sqrt{2}/4 \\ &\Gamma_{\rm rel} \to \Gamma_-/\sqrt{2}; \qquad w_+/\rho_+ \to 2\sqrt{2}\Gamma_-/3 \end{aligned} \tag{30}$$

[using Eq. (15]. For a parallel shock, where $b_- = b_+$, the Alfvénic Mach number is

$$M_{\rm A\pm} = \frac{v_\pm}{b}\left(\frac{w_\pm}{\rho_-} + b^2\right)^{1/2} \tag{31}$$

A switch-on shock occurs if the upstream flow is super-Alfvénic and the hydrodynamic jump conditions give a sub-Alfvénic downstream speed, which means, in the ultrarelativistic approximation,

$$\sqrt{1+b^2} < \Gamma_- < \sqrt{3}b \tag{32}$$

This parameter range is unusual, since it requires a plasma in which the magnetic field energy density greatly exceeds the rest mass energy density, as well as a shock front whose normal is closely aligned with the upstream magnetic field.

† Lichnerowicz [24] has pointed out that also the switch-on (and the switch-off) shock is not evolutionary. The physical reason for this is that the plasma cannot break the azimuthal symmetry around the direction of the magnetic field in order to create the transverse component. However, for an arbitrarily small angle between the shock normal and magnetic field, this symmetry is broken, and a shock appears which is both evolutionary and arbitrarily 'close' to the switch-on shock. On the other hand, the purely hydrodynamic solution does not have an evolutionary shock in its neighbourhood, when conditions (24) and (25) are violated [10].

(iii) The ultra-relativistic approximation is more commonly encountered in connection with perpendicular shocks, such as are thought to occur in the winds driven by radio pulsars such as the Crab [25, 12, 26, 27]. Here it is convenient to use the (Lorentz invariant) parameter

$$\begin{aligned}\sigma &\equiv \frac{B^2}{4\pi w} \\ &= \rho_- b^2/w \end{aligned} \tag{33}$$

which, in the case of a magnetic field orientated perpendicular to the flow, is just the ratio of the energy flux carried by the electromagnetic field to that carried by the particles. Kennel & Coroniti [26] have given an approximate solution for strong, ultrarelativistic perpendicular shocks:

$$\begin{aligned}\Gamma_+^2 &= \frac{8\sigma_-^2 + 26\sigma_- + 17 + \sqrt{64\sigma_-^2(\sigma_- + 1)^2 + 20\sigma_-(\sigma_- + 1) + 1}}{16(\sigma_- + 1)} \\ \frac{b_+}{b_-} &= \frac{\rho_+}{\rho_-} = \frac{\Gamma_-}{\sqrt{\Gamma_+^2 - 1}} \\ \frac{w_+}{\rho_+} &= 1 + \frac{\Gamma_-}{\Gamma_+}\left[1 + \sigma_-\left(1 - \frac{\Gamma_+}{\sqrt{\Gamma_+^2 - 1}}\right)\right]\end{aligned} \tag{34}$$

which goes over into the hydrodynamic solution (15) and (29) for $\sigma_- \to 0$.

As pointed out by Kundt & Krotscheck [12], the compression which can be obtained in a relativistic shock decreases as the magnetic field becomes more and more important dynamically. To illustrate this point we present in figure 1 the jump conditions solved for the case of a magnetic field at an angle of 45^{o} to the shock normal in the upstream frame. The shock is taken to be strong, in the sense that the pressure of the plasma upstream is negligible. However, we allow for an appreciable magnetic pressure in the upstream plasma, as measured by the Alfvénic Mach number, defined as $M_{\mathrm{A}} = v_-/v_{\mathrm{A}}$, with the (relativistic) Alfvén speed given by equation (22). The Synge equation of state is used in these computations, and at Alfvén Mach numbers above 100, the result is close to the hydrodynamical case. In addition, figure 1 shows the hydrodynamic result for a strong shock using the fixed adiabatic index approximation of equation (15), and taking the ultrarelativistic value $\hat{\gamma} = 4/3$ (which, of course deviates significantly from the Synge equation of state in the non-relativistic case).

These computations were performed using an algorithm based on the description in Appendix B. They extend the results presented by Ballard & Heavens [28] by using the Synge equation of state and showing explicitly that the division between super- and subluminal shocks used in that paper (and discussed in Section 3) is unimportant for the jump conditions. Similar results, but in terms of the parameter $\sigma_- = v_-^2/(M_{\mathrm{A}-}^2 - v_-^2)$, are given for the ultra-relativistic perpendicular shock by Kennel & Coroniti [26].

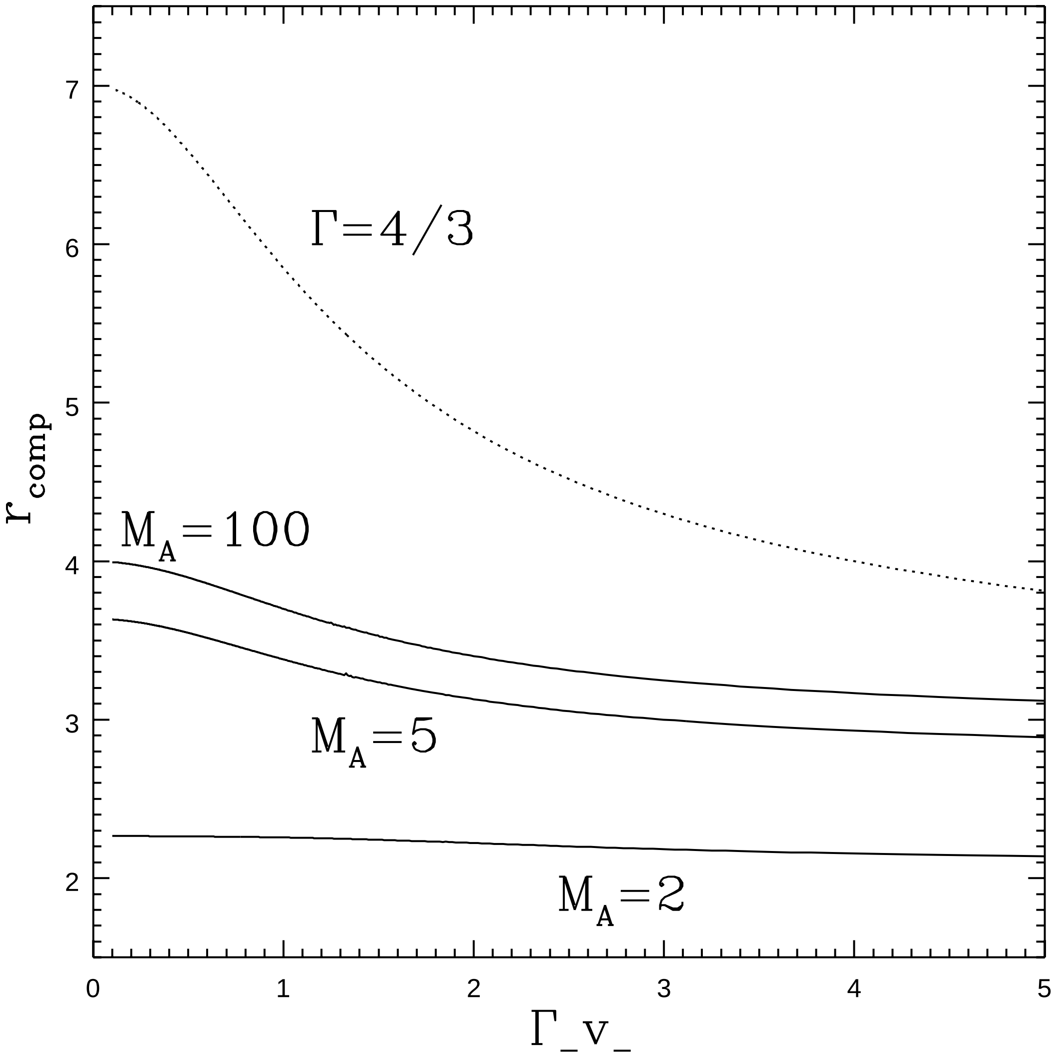

Figure 1. The compression ratio of a strong oblique fast-mode shock front ($\Phi_- = 45^o$) propagating into a magnetised plasma. Various Alfvén Mach numbers $M_{\rm A}$ are shown, together with the hydrodynamic approximation of equation (15) (dotted line).

3. Particle acceleration

Restricting ourselves to the picture of a shock front as a discontinuity in an MHD flow, the crucial question to be answered before particle acceleration can be discussed is the precise nature of the interaction between accelerated particles, the plasma and its embedded magnetic field. The standard starting point is orbit theory. Provided the embedded magnetic field varies slowly in time and space compared to the gyro-frequency and gyro-radius of the particle, the orbit can be described by the location of the gyro-centre (three spatial coordinates) the energy, the first adiabatic invariant or magnetic moment and the gyro-phase. The latter, which is the angle variable corresponding to the action variable 'magnetic moment', varies on the fastest time-scale. Correspondingly, it is assumed that the distribution function quickly adjusts itself to be independent of this coordinate. From this 'unperturbed' orbit, the effect of small fluctuations in the electromagnetic field can be taken into account using quasi-linear theory. The result is a transport equation which is a second order partial differential equation describing diffusion in energy, magnetic moment ($= p(1-\mu^2)/B$, where p is the momentum and μ the cosine of the 'pitch angle' between the velocity vector and the magnetic field) and a coordinate perpendicular to the magnetic field. Explicit expressions for the diffusion coefficients, which are applicable in the rest frame of the plasma, have been computed by several authors [29, 30, 31, 32]. The most important wave mode responsible for the fluctuations is thought to be the Alfvén wave propagating parallel to the magnetic field, since it is only weakly damped [33, 34]. In this case the fastest diffusion time-scale is that associated with pitch angle scattering. Terms involving diffusion in energy and in position of the gyro-centre are smaller. In the next step, it is assumed that pitch angle diffusion is rapid enough to keep the particle distribution function close to isotropy, which enables the transport equation to be reduced to one containing only diffusion in the spatial coordinate along the field line, together with smaller terms describing cross-field and energy diffusion [35, 36]. Neglecting diffusion in energy, one arrives at the well-known cosmic ray transport equation [37, 38]. Applying it to a flow pattern which contains a non-relativistic shock front leads to the theory of diffusive shock acceleration [39, 40, 41, 42].

This acceleration mechanism has been intensively studied (for reviews see Drury [43] and Kirk et al. [44]). At a non-relativistic shock wave for which v_- and v_+ are each very much less than the particle speed $v_{\rm p}$, the particle distribution at the shock is, to lowest order in $v_\pm/v_{\rm p}$, isotropic when viewed in either the upstream or downstream frames. A particle which crosses from upstream to downstream and back again then undergoes a small fractional increase in its momentum which is proportional to $v_{\rm rel}/v_{\rm p}$ and is given by $\Delta p/p = 4(v_- - v_+)/3v_{\rm p}$. The factor 4/3 is a consequence of isotropy. The only process which can stop this slow but inexorable acceleration is escape of the particle from the vicinity of the shock. With $n_{\rm s}$ the number density of particles at the shock the flux of (isotropic) particles of speed $v_{\rm p}$ crossing the shock is $n_{\rm s}v_{\rm p}/4$. Diffusion and isotropy guarantee that the number density of particles is constant in the downstream region so that the flux of escaping particles is then $n_{\rm s}v_+$. The probability of escape per shock crossing is then the ratio of the flux of escaping particles to those crossing the shock, $P_{\rm esc} = 4v_+/v_{\rm p}$. The ratio of $P_{\rm esc}$ to $\Delta p/p$ determines the slope of the integral particle spectrum (i.e. the number of particles above a momentum p). The phase space density of particles then has a power law spectrum $f(p) \propto p^{-q}$ where $q = -P_{\rm esc}/(\Delta p/p) - 3$.

This gives a spectral index, *which depends on the compression ratio of the shock alone*, of $q = 3r/(r-1)$ where $r = v_-/v_+$. Note that this result does not depend on the level of scattering as long as that scattering is diffusive leading to an isotropic distribution when seen in each fluid frame.

Relativistic flow brings substantial changes to this picture, because the assumptions made in deriving the spatial diffusion equation are no longer valid. Thus, when $v_{\rm rel}$ is of order the velocity of light, the quantity $v_{\rm rel}/v_{\rm p}$ can no longer be small. The Lorentz boost linking the two frames significantly deforms the angular distribution of the particles, so that it cannot be nearly isotropic in both the upstream and downstream rest frames. Instead of assuming spatial diffusion, the angular dependence of the distribution function must be computed explicitly.

Nevertheless, one can gain some understanding by exploiting a key property of the quasi-linear approach – namely that diffusion across the field lines is ineffective – despite the fact that a firm theoretical basis is lacking in the relativistic case. This property implies that, to a first approximation, a particle's guiding centre remains fixed to a given field line except at points where its orbit cuts the shock front. The kinematic implications are severe. The pattern of successive crossings and re-crossings of the shock front as a result of diffusion *along* the field lines, becomes progressively more difficult to maintain as the obliquity of the shock increases, since a diffusing particle has to chase not the shock front, but the point of intersection of the shock front with the field line to which it is tied. Re-crossing becomes impossible when the intersection point moves with a speed greater than that of light, i.e., $v_{\rm int} \equiv v_-/\cos\Phi_- \geq 1$, and this divides shock fronts into two categories: subluminal ($v_{\rm int} < 1$) and superluminal ($v_{\rm int} > 1$). The jump conditions themselves (see Section 2) do not exhibit any special features at the change-over between sub- and superluminal shocks, however, there are interesting differences when one considers the properties of the two types of shock under Lorentz transformations. Thus, for subluminal shocks it is always possible to find a transformation to the de Hoffmann/Teller frame [6] in which the electric field vanishes everywhere. This is a convenient frame for computational purposes. In the case of superluminal shocks, no such simple frame can be found. The best that can be done is to transform to a frame in which the magnetic field is perpendicular to the shock normal, the shock is stationary, and the incoming flow is in the same plane as the shock normal and the magnetic field [43, 23]. Generally, if one assumes the direction of the magnetic field in the upstream plasma has no causal connection with the shock front, so that it is randomly oriented with respect to the shock normal, subluminal shocks will greatly outnumber superluminal ones in subrelativistic flows. On the other hand, in relativistic flows subluminal shocks will be rare, since they require orientation of the magnetic field to within an angle of $1/\Gamma_-$ of the shock normal.

At superluminal shocks, perturbations to the particle orbit are unimportant for acceleration when cross-field transport is neglected. However, even in the absence of fluctuations which scatter energetic particles, a shock front in a perfect fluid is capable of increasing the average energy of a distribution of particles incident upon it. Seen from the upstream rest frame, there exists an electric field in the downstream half-space simply because it is in motion (the $-\mathbf{v} \times \mathbf{B}$ field). A charged test particle can tap into this energy source if its gyrations through the regions of different magnetic field strength upstream and downstream cause it to drift along the shock front in the appropriate direction. This is usually called 'shock-drift' acceleration. It can be analysed by tracing a large number of orbits numerically. The relativistic version of this mechanism has been investigated in [23] and is described in Section 3.1.

In Section 3.2 we turn to the situation in which scattering does play an important role in the acceleration mechanism – i.e., the relativistic generalisation of the diffusive shock acceleration mechanism – and summarise the analytic and semi-analytic approaches to the problem. These involve the solution of the angular dependent transport equation assuming an explicit form for the pitch angle scattering coefficient. As such, they neglect cross field transport and apply principally to subluminal shocks. However, these methods may also be applicable to the case in which no a priori assumption is made concerning cross-field diffusion. If the direction of the embedded magnetic field is unimportant because a particle performs only a fraction of gyration between shock crossings (as in the case of an ultra-relativistic shock), or because the fluctuations in the field strength reach or exceed the amplitude of the embedded field, then transport by successive small angle deflections can be treated simply by replacing the pitch angle by the angle between the *shock normal* and the particle velocity [45].

Despite the advantages of a semi-analytic approach, Monte-Carlo simulation provides the most popular technique for investigating acceleration at relativistic shocks. The formulation of the problem is conceptually simple, and the method permits one to look at a variety of effects (such as synchrotron losses and time dependence) which have so far defied an analytic approach. This work is discussed in Section 3.3.

The ideal MHD approach, coupled with a simple transport prescription for energetic particles allows us to make some predictions – such as spectral indices – which are, at least in principle, accessible to observation. Currently, the only work of which we are aware which goes beyond this picture concerns the structure of relativistic perpendicular shocks, with particular application to the Crab Nebula [46, 47, 48]. The techniques involved – one and two dimensional particle-in-cell or hybrid simulations – differ markedly from those employed in the perfect fluid case, and are not discussed in this review.

3.1. Shock-drift acceleration

The dramatic increase in surface brightness which can be produced by a relativistic shock front merely as a result of the 'compression' of the electrons was pointed out by P. Scheuer [49]. This raises the possibility that observations of hot-spots in extra-galactic radio sources could be understood even if the Fermi process with its emphasis on crossing and recrossing of the shock front were unimportant.

To quantify this statement, consider a gas of relativistic electrons with an isotropic distribution function in the local fluid frame. They achieve isotropy by experiencing elastic scattering by slowly moving, low-frequency MHD waves, which may be self-excited. The distribution in Lorentz factor γ is unaffected by the scatterings.

The phase space density of particles contained in the interval dp around p is conventionally assumed to be a power law:

$$f(p) = Cp^{-s} \tag{35}$$

between a lower and an upper cut off: $p_{\rm min} < p < p_{\rm max}$. The corresponding number density within this range of p is $n(p) = 4\pi p^2 Cp^{-s}$. Let us assume that this distribution with $C = C_-$ accurately describes particles in a fluid element which flows into an MHD shock.

If the scattering events are so rapid that the length scale over which they isotropise the electrons is much shorter than the length scale characterising the thickness of the shock, then the relativistic electrons react adiabatically. The Fermi process is unimportant in this case because scattering anchors the particles in the local fluid element and prevents them from repeatedly sampling the velocity difference between the upstream and downstream sides of the shock in between scatterings. The characteristics of the transport equation are then

$$p\rho^{-1/3} = \text{constant} \tag{36}$$

where ρ is the proper fluid density (e.g., [44]), so that downstream of the shock front one has

$$\begin{aligned} f_+(p) &= f_-[p(\rho_+/\rho_-)^{1/3}] \\ &= C_- \left(\frac{\rho_+}{\rho_-}\right)^{s/3} p^{-s} \end{aligned} \tag{37}$$

Provided p is far from the cut-off momenta, this can be written in terms of a (proper) compression ratio for the electron distribution $R_{\rm e}$:

$$R_{\rm e} \equiv \frac{f_+(p)}{f_-(p)} \tag{38}$$

$$= R^{s/3} \tag{39}$$

where R is the proper compression ratio of the MHD fluid.

Even if they are not scattered whilst traversing the shock, charged particles may still be said to behave 'adiabatically' in the sense that the first adiabatic invariant of motion (the magnetic moment) is conserved. For this approximation to be valid, it suffices that the length scale on which the magnetic field and fluid speed change (i.e., the shock thickness) is long compared to the gyro-radius of the electron concerned.

Perhaps surprisingly, the magnetic moment is still conserved to a good approximation even if the magnetic field changes discontinuously. This was pointed out by Parker [50] and Schatzman [51] for perpendicular shocks and investigated numerically by Decker [52]. From the work of Whipple et al [53] it is known that the magnetic moment is conserved during encounter with a discontinuous change in the magnetic field at a perpendicular shock front provided the velocity of the front is small compared to that of the electron. In the case of synchrotron emitting electrons, this means $v_- \ll 1$. Away from the shock front (i.e., further than a gyro-radius from it) the particle distribution may relax slowly to isotropy as a result of pitch angle scattering. However, crossing and re-crossing is ruled out if the shock is superluminal, in which case this process operates undisturbed by the Fermi mechanism. The effective compression ratio for the electron distribution defined in equation (38) is straightforward to calculate using Liouville's theorem applied to the drift-kinetic equation (e.g., [23])

$$R_{\rm e} = \frac{1}{2} R_{\rm B}^{(s-1)/2} \bar{\omega}^{-1/2} B_{\bar{\omega}} \left(\frac{1}{2}, \frac{s-1}{2}\right) \tag{40}$$

$$\approx \sqrt{\frac{\pi}{2}} R_{\rm B}^{(s-1)/2} \frac{\Gamma((s-1)/2)}{\Gamma(s/2)} \quad \text{for } R_{\rm B} > 3 \tag{41}$$

where $R_{\rm B}$ is the proper compression ratio of the magnetic field, $\bar{\omega} = (R_{\rm B} - 1)/R_{\rm B}$ and $B_{\bar{\omega}}(a, b)$ is an incomplete Beta function ([54], page 944). The special case $s = 4$ can be expressed in terms of elementary functions, and is given by van der Laan [55]. If the magnetic field is dynamically unimportant, the magnetic compression R_B is given by (29).

At a relativistic shock, the magnetic moment of a charged particle is in general not even approximately conserved, although for subluminal shocks there still exists a small region of phase space for particles moving with the shock front within which the approximation holds [56]. Notwithstanding this, significant progress can only be made by numerically following individual particle trajectories as they are carried over the shock front. Since those sections of the path between intersections are simply helices, the algorithm reduces to locating the intersection points and performing the relevant Lorentz transformations. Phase is now an important coordinate, so that results must be integrated over all initial phases, as well as initial pitch angles. The results presented in [23] show that the electron compression ratio $R_{\rm e}$ is much larger at relativistic shocks than a naive extrapolation of the non-relativistic results (39) and (41) would indicate. In fact, for $\Gamma_{\rm rel} \gg 1$, one has $R_{\rm e} \propto \Gamma_{\rm rel}^{s-2}$, compared to the asymptotic behaviours $R_{\rm e} \propto \Gamma_{\rm rel}^{s/3}$ and $R_{\rm e} \propto \Gamma_{\rm rel}^{(s-1)/2}$ predicted by equation (39) and equation (41), respectively. In connection with this result, it is interesting to note that at a strong relativistic shock front, the average Lorentz factor of *thermal* particles downstream is the same as their pre-shock value, as seen from the downstream rest frame. Essentially, the energisation in shock drift acceleration at an ultra relativistic shock front is only slightly greater than is achieved by isotropising the upstream particles using the downstream magnetic field and the static fluctuations associated with it.

Although each of the three mechanisms described in this section results in a strong enhancement of the energy density in accelerated particles, the boost in the energy of each individual particle is modest. The mechanisms work only when a population of particles with a non-thermal distribution flows in towards a shock front, and the characteristics, such as spectral index, of the incoming distribution are not changed. Thus, there is no characteristic spectral signature, nor is it possible by these mechanisms to accelerate a particle over several decades in energy. Nevertheless, these mechanisms would be the simplest ones to incorporate into a numerical hydrodynamic or MHD simulation.

3.2. First order Fermi acceleration - analytic and semi-analytic methods

In contrast to the shock-drift mechanism, the repeated crossings and re-crossings characteristic of first order Fermi acceleration enable large boosts in particle energy and, perhaps more importantly, produce a particle distribution with a characteristic spectral index. Early on, it was thought that the increased escape probability in the relativistic case would mean that most of the accelerated particles would be swept away from the shock never to return, which would severely reduce the acceleration 'efficiency' (i.e., cause the spectrum to fall off rapidly to higher energies). However, this does not happen for two reasons. Firstly, the escape probability is related to the speed of the shock in the downstream rest frame. This quantity does not increase indefinitely as the shock becomes faster, but remains lower than the relevant wave speed. In the case of a hydrodynamic shock, the wave speed is that of sound, which cannot exceed $c/\sqrt{3}$. Secondly, the acceleration per shock crossing also increases as the shock becomes faster. In fact, there is no upper limit to this quantity, since a particle which encounters a shock head-on (i.e., whilst moving along the shock normal) and returns in the opposite direction suffers a fractional increase in energy which is of the order of $\Gamma_{\rm rel}^2$. However, the average fractional energy gain is a sensitive function of the angular distribution of the particles, and, as we shall see, this adjusts itself such that the competition between acceleration and escape results in a power-law spectrum which does not differ radically from the non-relativistic value.

To find the spectrum of particles accelerated by the first order Fermi process at a shock front it is necessary to solve the transport equation in the upstream and downstream media and match the solutions at the shock front. In contrast with the extensive analytic developments in the non-relativistic theory, only a few special cases have been solved for relativistic flows. The simplest of these, which is outlined below is the determination of the characteristic power-law index of test particles accelerated at a plane parallel shock front in which the fluid flows along the shock normal. This was first attacked by Peacock [57], who, however, did not solve the full transport problem, but assumed a particular angular distribution of particles in the downstream plasma. It was subsequently solved using an eigenvalue expansion technique [58]. This method has been generalised to treat acceleration at oblique shocks, employing the additional assumptions of conservation of magnetic moment upon crossing the shock, and neglect of cross-field transport processes [22]. Much harder spectral indices were found in these cases, largely as a result of the accumulation of particles swept up into a precursor by repeated reflections from the shock front [59, 60, 56]. These are ameliorated somewhat when account is taken of the weakening of the compression ratio of an oblique shock front by magnetic pressure [28], as shown in figure 1. Steeper spectra may also result if cross-field transport becomes important.

'Modified' (parallel) shocks – i.e., those of finite thickness and a prescribed velocity profile formed the subject of another generalisation of the method [61, 62]. The technique described in the latter paper is relevant for the problem of injection at non-relativistic shocks, where the anisotropy of the particle distribution plays a key role [63]. Adding a term describing large-angle scattering to the transport equation allows further insight into the acceleration mechanism and its sensitivity to the scattering operator using essentially the same technique [64]. Non-linear effects, which play a prominent role in non-relativistic theory, have proved difficult to treat analytically – the only advance being the relativistic generalisation [65] of the classification of possible stationary solutions given in the diffusive case by Drury and Völk [66].

Returning to the problem of test particles at a parallel shock, in the presence of pitch angle diffusion described by the coefficient $D_{\mu\mu}$, but neglecting as usual diffusion in energy, the equation to be solved is

$$\Gamma_\pm(1+v_\pm\mu)\frac{\partial f}{\partial t}+\Gamma_\pm(v_\pm+\mu)\frac{\partial f}{\partial x}=\frac{\partial}{\partial\mu}D_{\mu\mu}\frac{\partial f}{\partial\mu}\ , \qquad (42)$$

where we have assumed the Lorentz factor of the particles is much larger than that of the flow and have accordingly replaced their velocity with the speed of light (= 1). The relatively simple form of (42) is a consequence of a mixed coordinate system [67] in which the cosine of the pitch angle μ is measured in the local rest frame of the plasma, but the space-time coordinates x and t refer to the rest frame of the shock front. Seeking a stationary solution in the shock frame, we separate the variables μ and x to find an expression for the general solution in terms of an eigenfunction expansion:

$$f = \sum_{i=-\infty}^{\infty} g_i(p) Q_i^v(\mu) \exp(\Lambda_i^v x/\Gamma), \quad , \tag{43}$$

where the $g_i(p)$ are arbitrary functions of momentum. This solution is valid in both the upstream ($x < 0$, $v = v_-$) or downstream ($x > 0$, $v = v_+$) regions. The eigenvalues Λ_i^v and eigenfunctions $Q_i^v(\mu)$ appropriate to each half space are solutions of the equation

$$\frac{\partial}{\partial \mu} D_{\mu\mu} \frac{\partial}{\partial \mu} Q_i^v(\mu) = \Lambda_i^v (v + \mu) Q_i^v(\mu) \quad . \tag{44}$$

together with the boundary conditions that the eigenfunctions be regular at the singular points $\mu = \pm 1$ [58].

The eigenvalue problem equation (44) resembles the standard Sturm-Liouville problem familiar in many branches of physics and shares with it several convenient properties ([68], page 227), such as a discrete spectrum with eigenvalues ordered according to the number of nodes displayed by the corresponding eigenfunction. However, the special feature of equation (44) is that precisely at that value of μ at which particles are stationary with respect to the shock front, the 'weighting function' $v_\pm + \mu$ changes sign. As a result, there are *two* families of eigenvalues and eigenfunctions for each value of v: one of them has positive, the other negative eigenvalues Λ_i^v. It is convenient to use the label i to indicate this, choosing positive integers for the positive eigenvalues and negative for the negative ones. The number of nodes possessed by the eigenfunctions is then $|i| - 1$. In addition to the two families of eigenvalues, there exists a special isotropic eigenfunction with zero eigenvalue which is labelled by $i = 0$: $\Lambda_0^v = 0$, $Q_0^v(\mu) =$constant. This just reflects the property that pitch angle diffusion tries to drive any distribution towards an isotropic one, which is the only stationary solution of the transport equation in the absence of boundary conditions at finite x. The eigenfunctions are orthogonal and may be normalised such that

$$\int_{-1}^{+1} \mathrm{d}\mu Q_i^v (v + \mu) Q_j^v = \eta_{ij} \tag{45}$$

where $\eta_{ij} = 0$ for $i \neq j$, $\eta_{ii} = 1$ for $i \leq 0$ and $\eta_{ii} = -1$ for $i > 0$.

In general, it is necessary to use a numerical technique to solve equation (44). Both a Galerkin method [58, 69] and a shooting method [70] have been employed. In the limiting cases of non-relativistic flow $v \ll 1$ and ultrarelativistic flow $v \to 1$, approximate analytic expressions are available, which are described in Appendix C

In the presence of a shock front at $x = 0$, the general solution equation (43) indicates that, in the upstream half-space ($x < 0$), all terms containing eigenfunctions with $i < 0$ diverge at large distance from the shock ($x \to -\infty$). Thus, for a physically admissible solution, the coefficients $g_i^-(p)$ must vanish for $i < 0$. Furthermore, if we are interested in particles accelerated by the shock front, we can demand that the density vanish far upstream, which implies that the coefficient with $i = 0$ must also vanish. Similar arguments can be applied to the downstream distribution, which, however, has non-vanishing density at $x \to \infty$.

To find an approximation to the characteristic power-law index, one assumes $f \propto p^{-s}$, so that in equation (43) $g_i(p) = p^{-s}$, and uses as an Ansatz an approximation to the downstream distribution which fulfills the boundary conditions at $x \to \infty$.

$$\tilde{f}(\tilde{p}, \tilde{\mu}, x) = \tilde{p}^{-s} \sum_{i=-J}^{0} \tilde{a}_i Q_i^+(\tilde{\mu}) \exp(\Lambda_i^+ x/\Gamma_+), \tag{46}$$

where the $\tilde{a}_i$ are constants, and we have truncated the expansion to include only a finite number $(J+1)$ eigenfunctions. We have also used the notation that the momentum and cosine of the pitch-angle measured in the downstream rest frame are $(\tilde{p}, \tilde{\mu})$. They are related to those measured in the upstream frame (p, μ) by a Lorentz transformation

$$\tilde{p} = \Gamma_{\rm rel} p (1 + v_{\rm rel}\mu) \tag{47}$$

$$\tilde{\mu} = \frac{\mu + v_{\rm rel}}{1 + v_{\rm rel}\mu}, \tag{48}$$

The distribution function expressed as a function of downstream quantities is denoted by $\tilde{f}$. On crossing the shock, particles are assumed not to undergo a sudden change in momentum (or direction of motion) so that Liouville's theorem demands continuity of the distribution. This condition reads

$$f(p, \mu, x = 0) = \tilde{f}(\tilde{p}, \tilde{\mu}, x = 0) \tag{49}$$

Accordingly, the upstream distribution at the shock front, $x = 0$, may be computed from equation (46) by substituting for $\tilde{p}$ and $\tilde{\mu}$ using equations (47) and (48). One must now try to fit the upstream boundary conditions as well as possible using the $J+1$ constants and the power-law index s. Although $\tilde{f}$ of equation (46) cannot be required to be orthogonal to *all* the upstream eigenfunctions which cause divergent behaviour at $x \to -\infty$, it can at least be made orthogonal to those J of them with the longest range (i.e., smallest $|\Lambda|$). Projecting onto these gives:

$$\Gamma_{\rm rel}^{-s} \sum_{j=-J}^{0} \int_{-1}^{+1} d\mu\, Q_i^-(\mu)(v_- + \mu)(1 + v_{\rm rel}\mu)^{-s} Q_j^+(\tilde{\mu})\, \tilde{a}_j$$
$$= 0 \tag{50}$$

for $i = -J \ldots 0$. The condition that the set of $J+1$ homogeneous equations (50) possess a non-trivial solution is sufficient to determine the unknown power-law index s. Once this is determined, the coefficients $\tilde{a}_j$ and hence the angular dependence of the distribution follow.

An example of the angular distribution at a relativistic shock, as seen from the rest frame of the downstream plasma, is shown in Fig. 2. This figure was computed

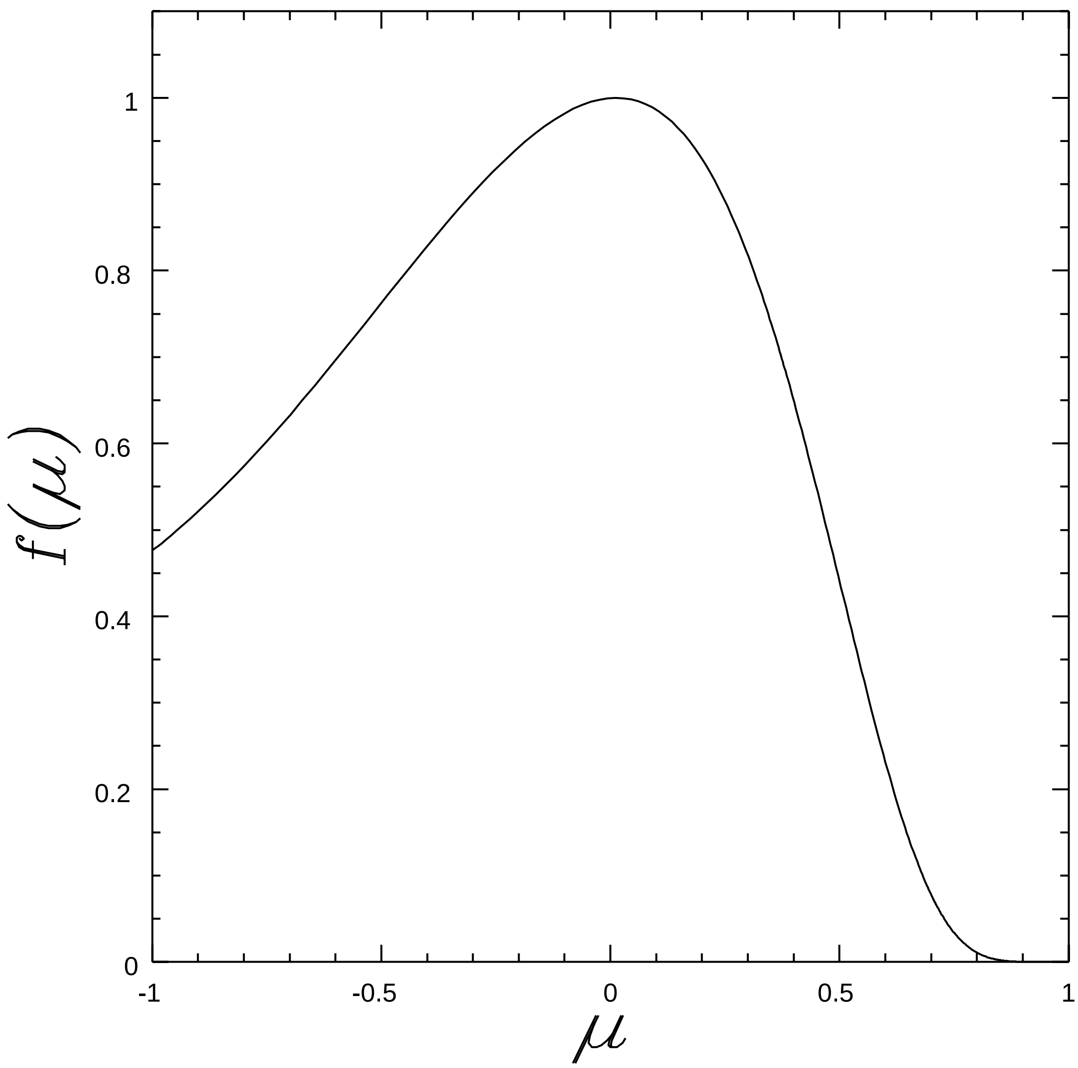

Figure 2. The pitch-angle distribution of accelerated particles at a parallel relativistic shock front with $v_- = 0.9$, and $v_+ = 0.37$, as a function of the cosine μ of the pitch angle measured in the rest frame of the downstream plasma. Isotropic pitch-angle diffusion is assumed and the normalisation of f is arbitrary. The depletion of particles with $\mu \approx 1$, (those which move almost along the shock normal into the downstream plasma) arises because particles which move into the upstream plasma are overtaken again by the shock before undergoing substantial deflection [45].

using an isotropic pitch-angle diffusion coefficient $D_{\mu\mu} \propto 1 - \mu^2$. As well as confirming that the the distribution is strongly pitch-angle dependent, Fig. 2 shows that very few particles travel in the direction $\mu = 1$, i.e., along the shock normal into the downstream region. The reason is that a particle which crosses into the upstream plasma undergoes relatively little deflection before being caught again by the relativistically moving shock.

Results for the power-law index s obtained by Kirk [69] are summarised in Fig. (3), where the characteristic spectral index is plotted as a function of $v_-\Gamma_-$ for parallel shocks having various equations of state. The plasma composition in this case is approximately primordial, with 25% helium by mass. Heavens and Drury [70] have given approximate formulae for s which they found by fitting their results in the range $0 < v_- < 0.98$. For isotropic pitch angle diffusion and a gas consisting of electrons and protons in thermodynamic equilibrium, they find for a strong shock

$$s \approx 3.99 - 3.16v_- + 10.86v_-^2 - 15v_-^3 + 7.46v_-^4 \tag{51}$$

This fit is also shown in Fig. 3. The agreement between the two treatments is clearly very good; the minor differences probably being due to slight variations in the jump conditions brought about by the different plasma compositions.

The main features of the plot can be understood as simply being due to the different compression ratios which arise when the shock fronts become relativistic. Nevertheless, significant deviations from a naive extrapolation of the non-relativistic formula $s = 3r/(r - 1)$ are found already at quite low speeds, as is shown in Fig. (4).

In contrast to the diffusive case, the value of the spectral index s for relativistic shocks depends on the functional form of the pitch-angle diffusion coefficient $D_{\mu\mu}$. This point has been investigated by Heavens and Drury [70] and by Kirk [69]. For example, if pitch-angle scattering through the point $\mu = 0$ is severely restricted [71], the spectrum is steepened. Figure 5 illustrates this for pitch-angle scattering given by

$$\begin{aligned} D_{\mu\mu} &\propto (1 - \mu^2)\mu^q \qquad \text{for } |\mu| > \epsilon \\ D_{\mu\mu} &= \text{constant} \qquad \text{for } |\mu| < \epsilon \end{aligned} \tag{52}$$

with $\epsilon = 1/30$ and the index q, which corresponds to the power-law spectrum of the turbulent wave-energy in the quasi-linear theory equal, taken in this example to be 2. Heavens and Drury, on the other hand adopt the prescription

$$D_{\mu\mu} = (1 - \mu^2)(\mu^2 + 0.01)^{1/3} \tag{53}$$

which roughly corresponds to the quasi-linear result in the presence of Kolmogorov turbulence.

To date, the method has been applied to shocks moving with a maximum Lorentz factor $\Gamma_- = 5$. Although the results in Fig. 3 seem to indicate a convergence to a value around 4.2 – a result also found and commented upon by Heavens and Drury [70] –

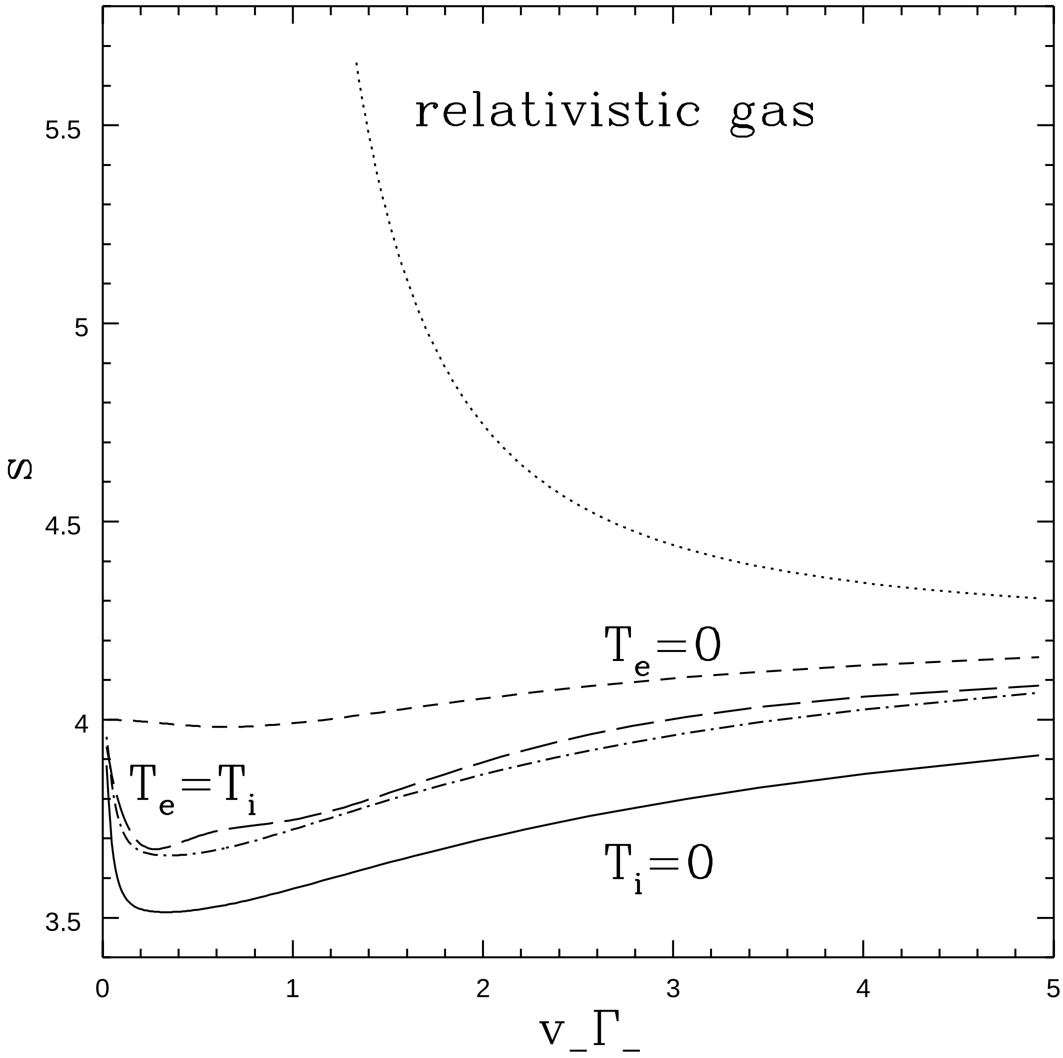

Figure 3. The spectral index as determined using the Q_J method for a parallel relativistic shock in plasma with various equations of state. Plotted on the abscissa is the x component of the four velocity of the upstream plasma $v_-\Gamma_-$. The dotted line corresponds to a relativistic gas with jump conditions given by equation (14). The dashed line depicts a gas consisting of fully ionised hydrogen and helium (25% by mass) with the electrons assumed cold ($T_\mathrm{e} = 0$); the solid line the same gas but with cold ions ($T_\mathrm{i} = 0$, i.e., dominated by electron pressure). Two sets of results are shown for complete thermodynamic equilibrium ($T_\mathrm{e} = T_\mathrm{i}$), those of Kirk [69] (dashed-dotted line) for the same composition as the other cases and those of Heavens & Drury [70] for a proton/electron gas (long dashed line), as given by equation (51).

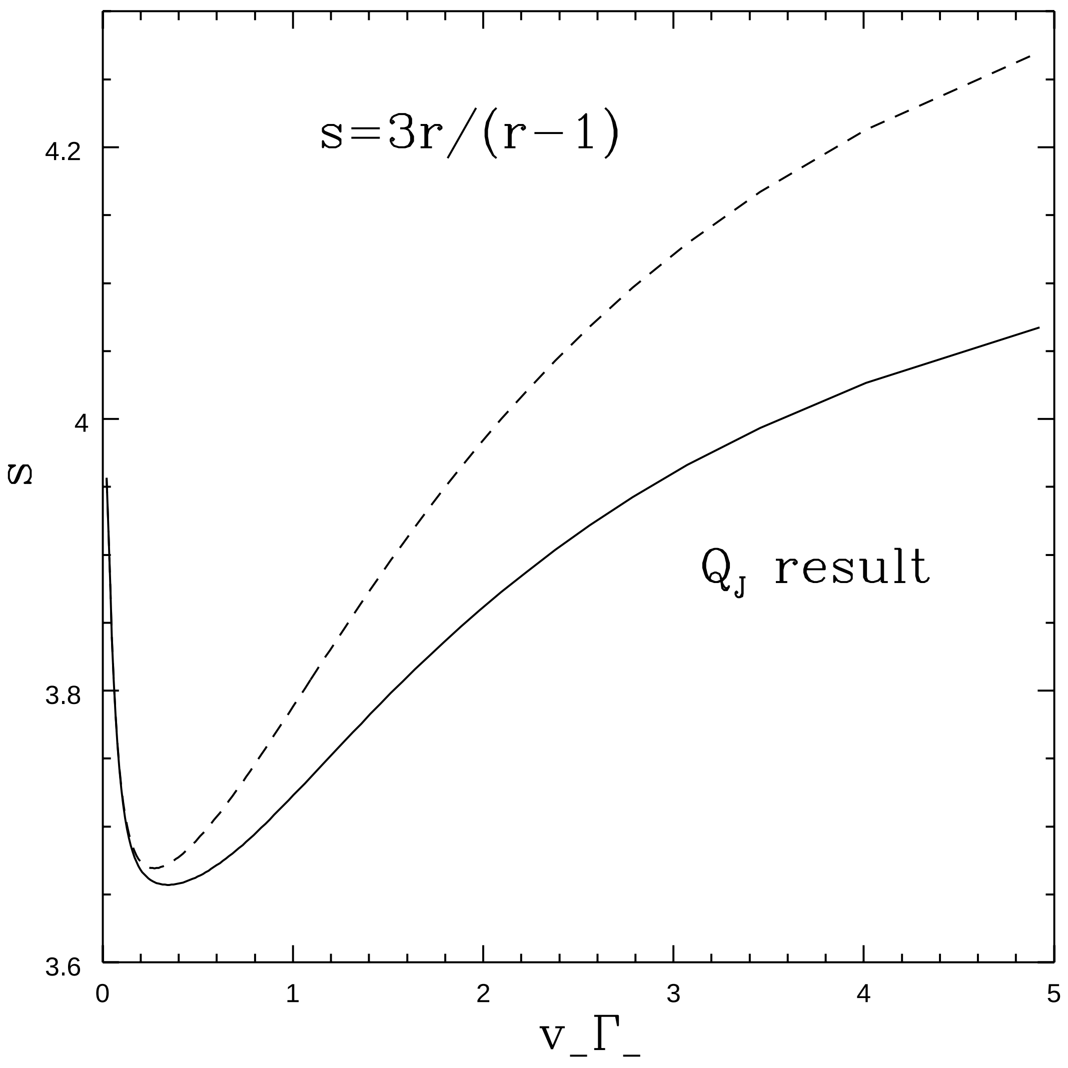

Figure 4. The spectral index as determined using the Q_J method (solid line) for a parallel relativistic shock in plasma (25% helium) in full thermodynamic equilibrium. The dashed line corresponds to the non-relativistic formula for the spectral index: $s = 3r/(r-1)$, where $r = v_-/v_+$ is the compression ratio

there is no analytic guarantee that the asymptotic limit either exists or is approached smoothly. Notwithstanding this, recent numerical results ([72, 45] – see section 3.3) also find convergence to $s = 4.2$ for very large Lorentz factors.

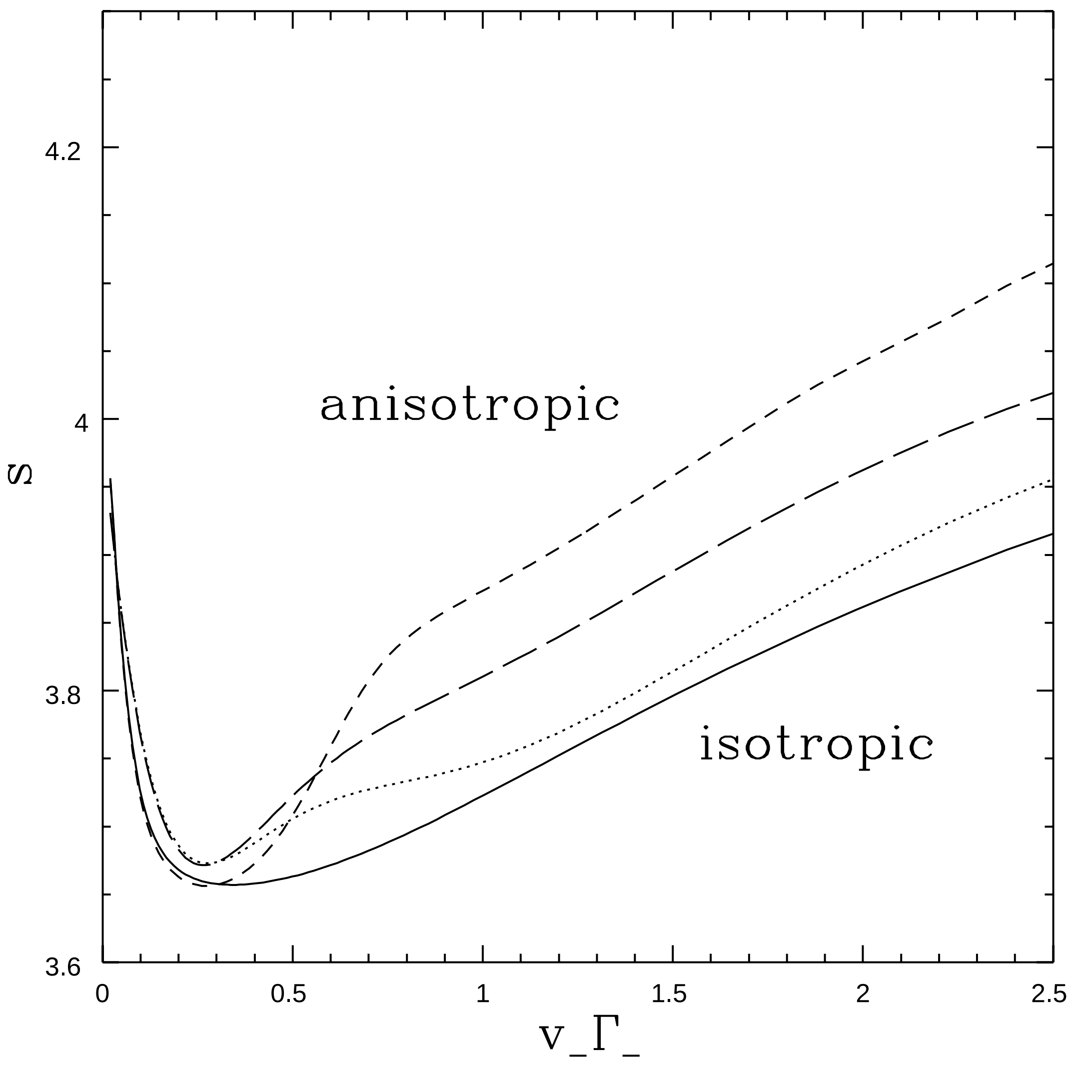

Figure 5. The effect of anisotropic pitch angle diffusion on the spectral index produced by a parallel relativistic shock front. The full line (isotropic) and the short dashed line (anisotropic) show the results of the Q_J computation [69], with, for the latter, pitch angle diffusion given by equation (52). The spectral index found by Heavens and Drury [70] is shown by the dotted line (isotropic) and long dashed line (anisotropic). The pitch angle diffusion coefficient in the latter case is given by equation (53). Note that [69] and [70] assume slightly different compositions for the plasma.

3.3. *Numerical treatments of acceleration*

3.3.1. Simulation of magnetic field The transport of charged particles in a relativistic flow can be simulated in a number of different ways. At perhaps the most basic level, the entire electromagnetic field can be specified in the relevant regions of space, and the particle orbits integrated directly. The basic idea behind this approach is that the waves responsible for the transport of energetic particles are low-frequency, MHD modes, with phase velocities much smaller than the velocity of the shock front. In this case, it seems a reasonable approximation to neglect any time dependence of the electromagnetic field, apart from that associated with the fast-moving discontinuity which is the shock front itself. A single realisation of a stochastically generated static magnetic field configuration is then sufficient to determine the motion of all particles.

This method has been employed by two groups to investigate particle acceleration at relativistic shocks [73, 74], with contradictory results. There are several problems with the method. The most severe of these is the limited dynamic range available for simulation of the stochastic magnetic field. Ballard & Heavens [73] use a 3-dimensional turbulent field with vanishing average component, generated by waves of random phase and intensity over a wavelength range of a factor of 100. Thus, a particle which during acceleration changes its gyro-radius by more than this factor will feel the effects of the limited dynamic range of the wave turbulence. Such a small energy range means that the characteristic index of the power-law spectrum expected of a realistic system can be determined only very approximately. Ostrowski [74], on the other hand, uses a larger dynamic range, but employs only a total of nine tranverse modes covering three orders of magnitude in spatial scale. He presents results for several orientations of the average magnetic field with respect to the shock normal. However, it is not clear that the acceleration process is independent of the number of wave modes used.

Inherent in each of these methods is another difficulty: suppose that we succeeded in realising a stochastic magnetic field over a sufficiently wide range of length scales. How can we be sure that the numerical orbit integration reproduces the particle trajectories with sufficient accuracy? At first sight, this does not appear to be a serious problem. However, recent studies of anomalous transport regimes in fusion plasmas (e.g., Rax & White [75]) and in the non-relativistic acceleration problem [76] show that the property of reversibility of a particle trajectory in a static magnetic field is both difficult to achieve numerically and important for the determination of the characteristic spectral index in shock acceleration. The problem can be understood by considering the situation when long wavelength fluctuations create a local magnetic configuration in which a particle is ‘trapped’. When such a structure passes over the shock front, the energy gained by a trapped particle depends strongly on how effectively the particle is confined [77]. Physically, one might expect the perturbing effect of non-static field fluctuations to play a role. This can be interpreted as an effective 'decorrelation time' over which the particle forgets about a particular realisation of the static stochastic field. Numerically, decorrelation is likely to be determined by the finite accuracy with which particle paths are computed. Because of the stringent requirements on accuracy, it has proved particularly difficult to devise numerical schemes which allow the study of the anomalous transport properties which arise on a time-scale shorter than the decorrelation time [75].

3.3.2. Simulation of particle transport An alternative, but perhaps less fundamental, approach to numerical simulation of acceleration is to make an assumption not about the stochastic field itself, but about the transport properties which it produces in the particles which are to be accelerated. This was a crucial step in developing the original analytic diffusive shock acceleration models. It results in a kinetic equation governing the single particle distribution function which contains a collision operator.

The basic idea of the Monte Carlo method is to find a way of constructing a stochastic trajectory whose distribution obeys the desired transport equation. Then, by repeating the procedure a large number of times, the distribution itself can be constructed approximately. This approach to solving transport problems has a long tradition, particularly in the fields of neutron transport and radiative transport. The transport of charged particles moving in a turbulent magnetic field is, however, qualitatively different, since the turbulence acts continuously to deflect the particle, whereas the scatterings of a neutron or photon are impulsive events which act on the trajectory during short time intervals between which are long periods of undisturbed flight. The differences are reflected in the mathematical properties of the collision operator contained in the transport equation. The pitch-angle diffusion operator

$$\mathcal{C}[f(\mu)] \equiv \frac{\partial}{\partial\mu} D_{\mu\mu} \frac{\partial f}{\partial\mu} \tag{54}$$

results in a transport equation which is a second order differential equation, for example that given in equation (42). This describes the continuous deflection of the particle by an infinite succession of infinitesimally small changes in pitch angle. On the other hand, the transport of photons and neutrons is described by scattering through a finite angle. In the simplest case of elastic scattering, one has, ignoring for the moment the gyro-phase,

$$\mathcal{C}[f(\mu)] \equiv \nu_{\text{scatt}} \left[\int_{-1}^{1} \mathrm{d}\mu' p(\mu,\mu') f(\mu') - f(\mu) \right] \tag{55}$$

where μ_{scatt} is the scattering frequency and $p(\mu,\mu')\mathrm{d}\mu$ is the probability that in a single scattering a particle with pitch angle cosine μ' is scattered into the range $\mathrm{d}\mu$ around μ.

The spectral properties of these two operators are quite different [64], as is the approach to constructing a corresponding stochastic trajectory. In the first case, one formally makes use of the Ito calculus (e.g., Gardiner [78]) to write a stochastic differential equation (SDE). The appropriate stochastic trajectory is then found by numerically integrating the SDE. An intuitive picture of this procedure is the following: to proceed from one point on a stochastic trajectory (labelled by, say x_i, μ_i) to the next, one must solve the transport equation under the initial condition $f(x, \mu, t = 0) = \delta(x - x_i)\delta(\mu - \mu_i)$. For small changes in x, this can be done approximately by assuming that μ changes only slightly. Expanding equation (42) in powers of $\mu - \mu_i$, one finds

$$\Gamma_\pm(1 + v_\pm\mu_i)\frac{\partial f}{\partial t} + \Gamma_\pm(v_\pm + \mu_i)\frac{\partial f}{\partial x} = D_{\mu\mu}(\mu_i)\frac{\partial^2}{\partial\mu^2}f + D'_{\mu\mu}(\mu_i)\frac{\partial}{\partial\mu}f \qquad (56)$$

where $D' = \mathrm{d}D/\mathrm{d}\mu$. The substitutions $\Delta = (t - t_i)/[\Gamma_\pm(1 + \mu_i v_\pm)]$, $\Xi = (x - x_i)/[\Gamma_\pm(v_\pm + \mu_i)]$ and $\eta = \mu - \mu_i + D'\Delta$ reduce this to the heat conduction equation, and the solution is easily seen to be

$$f[x, \mu, t = t_i + \Gamma_\pm(1 + \mu_i v_\pm)\Delta]) = \frac{\delta(x - x_i - \Gamma_\pm(v_\pm + \mu_i)\Delta)}{\sqrt{\pi D_{\mu\mu}\Delta}} \exp\left[-(\mu - \mu_i - D'_{\mu\mu}\Delta)^2/(D_{\mu\mu}\Delta)\right] \qquad (57)$$

The next point on the trajectory is found by setting a sufficiently small time step Δ and choosing a new stochastic value of μ from the Gaussian distribution of equation (57). This method, together with specialised techniques for enhancing the statistical significance of the results (such as the 'splitting' technique) was applied to the the acceleration problem for particles undergoing synchrotron losses in [79]. The Ito approach to more general problems including second order Fermi acceleration has been presented by Krülls & Achterberg [80].

Whereas the Fokker-Planck operator stems from the quasi-linear theory of plasma turbulence, as discussed in Sect. 3.2, there is currently no theoretical justification for a large-angle scattering operator such as equation (55) to describe charged particles propagating in a turbulent plasma. Nevertheless, motivated by the qualitative appearance of particle trajectories in simulations of strong plasma turbulence [81], which show sudden, large-angle deflections, a mixture of the two operators has been investigated analytically [64]. The motivation to perform Monte-Carlo simulations using the large-angle scattering operator is even stronger, since it is both relatively simple to implement and modest in its use of computer time. A stochastic trajectory is constructed by first choosing a scattering time distributed exponentially in the usual manner: $\Delta t = -\nu_{\mathrm{scatt}}\ln(\xi)$, where ξ is a random number distributed uniformly on the interval $[0, 1]$. During this interval, the particle propagates with unchanged pitch angle from position x_i to $x_{i+1} = x_i + (v_\pm + \mu_i)\Delta t$. The new value of $\mu = \mu_{i+1}$ is then found from the distribution $p(\mu, \mu_i)$. In the non-relativistic case, this method has proved highly popular (for a review, see [82]). Despite the lack of a theoretical background, the results it yields agree with solutions found using the diffusion approximation. This is because the distribution function in the non-relativistic case is close to being isotropic. Independent of the mathematical structure of the collision operator, it is then always possible to derive the equation of spatial diffusion, so that a Monte-Carlo simulation using equation (54) must yield the same results as one performed using the more economical operator equation (55).

Once the motion becomes relativistic (or, more generally, once the fluid speed approaches the particle speed), anisotropies arise, and, with them, differences between the pitch-angle diffusion and large-angle scattering cases [64, 83]. Nevertheless, large-angle scattering with complete isotropisation at each scattering (i.e., $p(\mu, \mu') = 0.5$) has been used to estimate the acceleration time at relativistic shocks [84, 83, 85, 86], a quantity which is needed in order to estimate the maximum energy cosmic rays which can be produced by the relativistic jet of a radio galaxy. It is, of course, possible to choose the large angle scattering operator such that not only the pitch angle is affected, but also the phase and, more importantly, the position of the guiding centre. Particles can then move across field lines as a result of scattering, mimicking the quasi-linear process of cross-field diffusion. This effect has been studied in connection with acceleration at non-relativistic oblique shocks [87]. If, in addition, the scattering is chosen to be strongly peaked in the forward direction, then pitch-angle diffusion is simulated. In this way, a comparison of the effects of pitch angle diffusion and large-angle scattering has been made in investigations of relativistic, oblique shocks, both with [60, 56] and without [59] explicit implementation of the assumption of magnetic moment conservation.

Monte-Carlo simulations have also been performed for highly relativistic shocks by Bednarz & Ostrowski [72] using upstream Lorentz factors up to roughly 240. They find the spectral index of accelerated particle converges to the value $s = 4.2$, independent of the orientation of the magnetic field, provided both pitch angle scattering and cross-field diffusion are permitted. However, in the ultra-relativistic limit, a particle which manages to cross a shock front from the downstream side into the upstream flow is very rapidly overtaken again once it is deflected. In fact, it can perform only a small fraction ($\sim 1/\Gamma_-$) of a gyration about the magnetic field line, unless the direction of the field is exactly along the shock normal [45]. In this case, the upstream transport cannot be represented by large-angle scattering. Instead, a combination of motion in a uniform field, and diffusion in angle due to fluctuations in the field on length scales much *shorter* than a gyro-radius arises. If the field fluctuates rapidly, one would expect to recover the operator equation (54), where now the quantity μ is interpreted not as the cosine of the pitch angle, but as the cosine of the angle between the particle velocity and the shock normal. Gallant et al [45] have extended the method to the ultra relativistic limit ($\Gamma_- \to \infty$) and considered both the case of diffusion in angle and scatter-free deflection by a uniform field. The corresponding power laws are $s = 4.25$ and 4.3 respectively, in reasonable agreement with Bednarz and Ostrowski, despite differences found in the angular distribution of the particles. This result is particularly encouraging for those theories of gamma-ray burst sources which use a relativistic blast wave to accelerate the particles, since it is close to the index of the particle spectrum required to produce afterglow spectra [88, 89].

4. Discussion

At the outset of this paper we pointed out that recent observations of blazars and gamma-ray bursts (GRBs) have each given renewed impetus to the study of particle acceleration in relativistic flows. We now address the issue of to what extent the results of these studies have been brought into contact with the observations of such objects.

Shock fronts arise when the relativistic flows encounter the ambient material. Variability in the central 'engines' of these sources may also result in internal shock waves, for example along the jets of AGNs. The shock jump conditions are then contained in the theory of section 2, at least at the MHD level, and, given some knowledge or model of the constituent matter and magnetic field, the possible shock configurations follow. In principle it is then possible to apply the acceleration theory of section 3 to model the energisation of highly relativistic particles. However, although reliable computations of flow patterns are now available, the most common approach to acceleration is still to assume a power law distribution of particles. In those instances where the acceleration is modelled at a deeper level it is usually with a simple phenomenological equation for the distribution [90, 91, 92, 93].

Before discussing the issues relating to jets and GRBs it should be noted that there exists in Nature one relativistic shock front which we are particularly well-placed to observe ions [25]. It is located in the Crab Nebula, and is responsible for thermalising the energy which streams from the central pulsar in the form of a relativistic flow of positrons and electrons, possibly contaminated by. It is thought that the shock is stationary and the magnetic field oriented perpendicular to the shock normal [26]. Using $1\frac{1}{2}$ D numerical simulations, a determined effort has been made to understand both the plasma physics of the shock front and the connection with particle acceleration. However, this source seems fundamentally different to gamma-ray blazars and gamma-ray bursts. Not only is it much less powerful, but it also does not display the rapid variability characteristic of the extra-galactic sources. In view of this, and because of the very different technical approach employed, we do not attempt to synthesise this theory into our discussion, but refer the interested reader to the original papers [46, 47, 48].

4.1. Relativistic Jets

The problem of how particles are accelerated to non-thermal energies in relativistic jets has been discussed for a number of years [94]. Diffusive acceleration at non-relativistic shocks is a possibility which appears to provide a reasonable picture of acceleration at several jet hot-spots which emit synchrotron radiation. In particular, the observed softening of the spectrum towards higher frequencies has been compared with analytic computations which include energy losses by synchrotron radiation [95, 96, 97]. However, both apparent superluminal motion and the rapid variability of emission from blazar jets imply substantial Doppler boosting, which indicates that the non-relativistic theory is inadequate.

The first attempt to model the radio emission of relativistic jets was made by Wilson and Scheuer [98], who performed numerical hydrodynamic simulations in which it was assumed that a fixed fraction of the energy thermalised at a shock front is converted into relativistic particles and magnetic fields. This is a rather sweeping assumption, covering not only particle acceleration, but also a dynamo process to convert part of the available energy into magnetic flux. Although such processes may well occur, there is currently no theoretical prospect of checking whether or not the assumed values of the parameters are realistic. Subsequent investigations have chosen to inject particles at a particular point and simply allow them to be compressed adiabatically at shock fronts according to Eq. (39) [99, 100, 101]. Since all of these are hydrodynamical schemes, which do not follow the evolution of the magnetic field, equipartition was assumed. If correct at injection, this assumption continues to hold through homologous compressions or expansions, but it is violated at a shock front. Of course, if the field is in some sense random, the average effect of a shock may be similar to homologous compression, but this is not going to be the case for sources with a high degree of polarisation. Only a rapidly acting dynamo (or, in some cases, reconnection) could then restore equipartition and thus rescue the simulations. Dropping the assumption of equipartition by assuming the fields to be frozen into the plasma (as in ideal MHD), Matthews and Scheuer [102, 103] have computed the emission patterns, once again assuming that relativistic electrons are compressed adiabatically at shock fronts. Although they enable interesting simulated ‘radio maps’ to be constructed, the major shortcoming of these simulations is that they do not include enough of the physics of particle acceleration to be able to predict spectra.

The best developed model of blazar spectra is based on the picture of a shock front moving down a jet [104]. Both the magnetic field and the particle distribution vary with position and the observed radiation is a superposition from different parts of the jet [105, 106]. These models are generally called ‘inhomogeneous’. However, recent results concerning the rapid variability of blazar sources at all frequencies [107] and the detection of their emission at energies up to at least 10 TeV [108] have provided new restrictions on the possible acceleration mechanisms. The observed simultaneous variations in X-rays and TeV gamma-rays indicate that a single population of particles in a relatively localised region is responsible. Consequently ‘homogeneous’ models have been widely discussed [109, 110, 111, 112, 93] and there is rough agreement on the parameters of the emission region. Furthermore, simultaneous variability of emission at widely differing wavelengths is more easily interpreted in terms of directly accelerated electrons than in hadronic models [113], where the high energy emission results from the acceleration of protons.

In the case of blazars the synchrotron emission in the radio to infra-red range typically displays a very hard power-law ($\alpha < 0.5$). For homogeneous models this means a flatter particle spectrum is needed than the canonical $s = 4$ result of non-relativistic theory, since the cooling time of the responsible particles is long, and the indices are related by $\alpha = (s-3)/2$. For Markarian 421, for example, a value of $s = 3.7$ is required to give the correct index of $\alpha \approx 0.35$ for the synchrotron emission. From Fig. 3, we see that, in the case of parallel shocks, such values are obtained only for mildly relativistic speeds in plasmas in which the electron pressure dominates. A perhaps more plausible alternative is to appeal to the fact that oblique relativistic shocks, through a combination of shock-drift and first-order Fermi acceleration, give much harder spectra ranging up to $s = 3$ [22]. This is due to the increased importance of reflections back into the upstream region from the shock front with increasing obliquity and shock speed, as discussed in section 3.2.

4.2. Fireball models of GRBs

The most popular, generic model for GRB sources is that of the fireball [114, 115, 116] which involves the sudden release of energy in the form of an optically thick $e^{\pm}$ plasma. While initially confined to a small volume, the plasma, and along with it the radiation, expands out to the point where the system becomes optically thin, releasing the electromagnetic radiation. The presence of a baryonic component can, however, result in the conversion of the initial internal energy into the kinetic energy of a thin shell of matter which expands relativistically, if such baryonic 'contamination' is small, into the surrounding medium [117]. When this shell interacts with the ambient medium a relativistic shock front forms which ultimately dissipates the kinetic energy of the ejecta into post-shock thermal energy and the production of energetic particles. In qualitative terms at least this picture is analogous to that of an expanding supernova remnant where the theory of diffusive shock acceleration can be applied. However, although the hydrodynamics of an expanding fireball have been well studied [14, 118, 119, 120, 121], the theory of particle acceleration at relativistic shocks, with the exception of some Monte-Carlo studies, has not been applied to these sources. This is also true of the case where a fluctuating Lorentz factor for the ejecta leads to the formation of internal shocks [122, 123]. Likewise, arguments favouring a common origin for ultra-high-energy cosmic rays and GRBs [124, 125] have used simple estimates of the acceleration processes which may take place. If the problem of acceleration is essentially treated as one of *injection* where a value of $s = 4$ is assumed and the total energy in energetic particles is parameterised as some fraction of the total fireball energy, estimates of the synchrotron and synchrotron self-Compton fluxes can be made [126, 127] and compared with observations. However, there are many important physical questions still unanswered. How does the environment and its equation of state influence the spectrum? Can a description of acceleration at multiple, internal shock waves account for the variability in GRBs?

It is not hard to see why the acceleration part of the problem has been largely simplified in the literature for GRBs. Until recently, published results were restricted to Lorentz factors of less than about 10, whereas GRBs require values ten times larger. First results have now appeared for the first-order Fermi process in the ultra-relativistic case [72, 45] and report a characteristic value of the power-law index encouragingly close to that which the observations seem to indicate [88, 89, 128]. As in the non-relativistic case, the compression ratio at an ultra-relativistic shock is independent of the shock speed. If, as the simulations suggest, the power-law index of accelerated particles turns out also to be independent of the shock speed, modelling of individual events will become simpler, and the theory of particle acceleration may play an important role in advancing our understanding these sources.

Acknowledgments

We are especially indebted to Y. Gallant and A. Heavens for a careful reading of the manuscript and a number of important suggestions. We also thank A. Achterberg and J. Lyubarskii for stimulating discussions. This collaboration was supported by the TMR programme of the European Commission under the network contract number ERBFMRX-CT-0168.

Appendix A. Hydrodynamic jump conditions

Consider a fluid made up of a number of constituents (electrons, protons and atoms of H and He, for example), labelled by the suffix i, and assign to each a temperature T_i. For an ideal gas of monatomic, non-degenerate constituents, the contribution w_i of each of them to the total enthalpy density is

$$w_i = m_i n_i G(m_i/T_i) \tag{A1}$$

where m_i is the rest-mass of the i'th constituent and n_i its proper number density. Note that we set the speed of light and Boltzmann's constant equal to unity $k_\mathrm{B} = c = 1$. The function $G(z)$ is given in terms of modified Bessel functions of the first kind (McDonald functions):

$$G(z) = \frac{K_3(z)}{K_2(z)} \tag{A2}$$

([129]), and has the asymptotic expansion for low temperatures

$$G(m/T) \to 1 + \frac{5T}{2m} \quad \text{as } T \to 0 \tag{A3}$$

and for high temperatures

$$G(m/T) \to \frac{4T}{m} + 1 \quad \text{as } T \to \infty \tag{A4}$$

Each constituent satisfies the ideal gas law

$$p_i = n_i T_i \tag{A5}$$

and the overall pressure, enthalpy density and energy density are simply

$$\begin{aligned} p &= \sum p_i \\ w &= \sum w_i \\ e &= w - p \end{aligned} \tag{A6}$$

We further define the rest-mass density ρ

$$\rho = \sum m_i n_i \tag{A7}$$

and the abundance (by mass) of the constituent i:

$$\eta_i = m_i n_i / \rho \tag{A8}$$

so that $\sum \eta_i = 1$.

The equation of state for this dissipation free (adiabatic) case is then

$$w = \rho \left[\sum \eta_i G(m_i/T_i) \right] \tag{A9}$$

together with a relationship between the T_i. (For example, in thermodynamic equilibrium: $T_i = T$, or, for cold electrons/hot ions: $T_{\rm e} = 0$, $T_{\rm H} = T_{\rm He} = T$.)

The speed of sound is simply given by $v_{\rm s}^2 = (\partial p/\partial e)_s$ where s is the specific entropy defined by the first law of thermodynamics: $T\mathrm{d}s = \mathrm{d}(e/\rho) + p\,\mathrm{d}(1/\rho)$. Using Eq. (3), and assuming $\hat{\gamma}$ to be constant, we obtain

$$v_{\rm s}^2 = \frac{\hat{\gamma} p}{\rho} \left[\frac{(\hat{\gamma} - 1)\rho}{(\hat{\gamma} - 1)\rho + \hat{\gamma} p} \right] \tag{A10}$$

which yields the familiar non-relativistic result for $p \ll \rho$ and gives $v_{\rm s} \to 1/\sqrt{3}$ for a relativistic gas.

The jump conditions Eqs. (7) and (8) can be simplified by the introduction of the following notation: let the quantities $\phi_\pm$ be defined by

$$\Gamma_\pm = \cosh\phi_\pm \,. \tag{A11}$$

Then one has

$$v_\pm = \tanh\phi_\pm \tag{A12}$$

The possibility of particle creation at the shock front may be taken into account by reserving the notation ρ_+ for the density of conserved particles, and introducing the parameter η to relate the total downstream rest-mass density $\rho_{\mathrm{total}+}$ to ρ_+:

$$\eta = \rho_+/\rho_{\mathrm{total}+} \tag{A13}$$

If particle number is conserved, $\eta = 1$, for small η, a large number of particles of non-zero rest-mass are created at the shock. In terms of the energy per unit rest mass $\bar{e}_- = e_-/\rho_-$ and $\bar{e}_+ = e_+/\rho_{\mathrm{total}+}$ and the similarly defined pressure per unit rest mass $\bar{P}_\pm$, one obtains

$$\begin{aligned}
\rho_+\sinh\phi_+ &= \rho_-\sinh\phi_- &\quad (\mathrm{A14})\\
(\bar{e}_+ + \bar{P}_+)\sinh^2\phi_+ + \bar{P}_+ &= \eta\frac{\rho_-}{\rho_+}\left[(\bar{e}_- + \bar{P}_-)\sinh^2\phi_- + \bar{P}_-\right] &\quad (\mathrm{A15})\\
(\bar{e}_+ + \bar{P}_+)\sinh\phi_+\cosh\phi_+ &= \eta\frac{\rho_-}{\rho_+}\sinh\phi_-\cosh\phi_-(\bar{e}_- + \bar{P}_-). &\quad (\mathrm{A16})
\end{aligned}$$

Elimination of ρ_+/ρ_- leads, after a little manipulation, to

$$\bar{w}_+\cosh\phi_+ = \eta\bar{w}_-\cosh\phi_- \tag{A17}$$

and

$$(\bar{w}_+\cosh^2\phi_+ - \bar{e}_+) = \eta\bar{e}_-\sinh\phi_+\sinh\phi_-\left(1 + \frac{\bar{P}_-\coth^2\phi_-}{\bar{e}_-}\right), \tag{A18}$$

where $\bar{w}_\pm = \bar{e}_\pm + \bar{P}_\pm$. The last term on the right-hand side of equation (A18) can be neglected if one restricts one's consideration to strong shocks, i.e. to shocks in which the upstream pressure is negligible. This approximation may be extended by assuming the upstream medium is cold, in which case the gas possesses only that energy attributable to its rest mass: $\bar{e}_- = 1$. Then, eliminating $\cosh\phi_+$, one has

$$\cosh^2\phi_- = \frac{\bar{w}_+^2(\bar{e}_+^2 - \eta^2)}{\eta^2(\bar{e}_+^2 - \eta^2 - \bar{P}_+^2)}, \tag{A19}$$

which is a generalisation to the case $\eta \neq 1$ of a relation found by Peacock [57]. Alternatively, one may obtain from Eqs. (A17) and (A18) the relation

$$\begin{aligned}
\bar{e}_+ &= \eta\cosh\phi_-\cosh\phi_+ - \eta\sinh\phi_-\sinh\phi_+\\
&= \eta\cosh(\phi_- - \phi_+) &\quad (\mathrm{A20})
\end{aligned}$$

The right-hand side of Eq. (A20) is just η times the Lorentz factor $\Gamma_{\rm rel}$ associated with the relative velocity of the upstream fluid with respect to the downstream fluid. Thus, in the absence of particle creation ($\eta = 1$), the average energy per particle as seen from the frame of the downstream fluid is constant across a strong shock (in which $\bar{e}_- = 1$). [130].

For a given upstream velocity v_-, equation (A19) must be solved numerically to give the downstream parameters. The procedure is as follows: v_- determines $\cosh\phi_-$ through Eq. (A11). The right-hand side of (A19) is a function of the single parameter $\bar{e}_+$ (the average Lorentz factor), since the pressure $\bar{P}_+$ is given through the equation of state Eq. (A9). A root finding algorithm can therefore be used to find $\bar{e}_+$. By means of equation (A17), which for strong shocks specialises to

$$\bar{w}_+ \cosh\phi_+ = \eta \cosh\phi_-, \tag{A21}$$

one finds the downstream velocity v_+.

The ultra-relativistic case is best considered without imposing the restriction to strong shocks. The equation of state $p = e/3$ can then be applied in both the upstream and downstream regions. Returning to equations (A17) and (A18), one finds, after a straightforward calculation,

$$v_- v_+ = \frac{1}{3}. \tag{A22}$$

A useful analytic expression for strong shocks can be found if the equation of state (3) is used [14]. The procedure is to write the specific enthalpy in terms of $\Gamma_{\rm rel}$ using Eq. (A20):

$$\bar{w}_+ = \hat{\gamma}(\eta\Gamma_{\rm rel} - 1) + 1 \tag{A23}$$

Remembering that $\bar{w}_- = 1$ for a strong shock, the $\cosh\phi_+$ term of Eq. (A17) can be rewritten as a function of $\phi_+ - \phi_-$ and ϕ_- to give an expression for $\tanh\phi_-$. Writing this in terms of $\Gamma_{\rm rel} = \cosh(\phi_+ - \phi_-)$ one finds

$$\Gamma_-^2 = \frac{\bar{w}_+^2(\Gamma_{\rm rel}^2 - 1)}{\hat{\gamma}(2-\hat{\gamma})(\eta\Gamma_{\rm rel} - 1)^2 + 2(\eta\Gamma_{\rm rel} - 1) + 1 - \eta^2} \tag{A24}$$

Thus, given η and the relative speeds of the upstream and downstream fluids, the shock speed and downstream pressure can be written down.

Appendix B. MHD jump conditions

In solving the MHD shock jump conditions it is useful to define the components of $b_\pm^\mu$ and $u_\pm^\mu$ along the shock normal, $d_\pm \equiv b_\pm^\mu l_\mu$ and $a_\pm \equiv u_\pm^\mu l_\mu$. These Lorentz scalars take the values $d_\pm = \Gamma_\pm (B_\pm/\sqrt{4\pi\rho_-}) \cos\Phi_\pm$ and $a_\pm = \Gamma_\pm v_\pm$. With $n_\pm = \rho_\pm/\rho_-$ the jump conditions become

$$
\begin{aligned}
&[na] &&= 0 \\
&[V^\alpha] &&\equiv [du^\alpha - ab^\alpha] = 0 \\
&[W^\alpha] &&\equiv \left[anGu^\alpha + \frac{n}{z}l^\alpha + |b|^2\left(au^\alpha + \frac{1}{2}l^\alpha\right) - db^\alpha\right] = 0
\end{aligned}
\tag{B25}
$$

where $z = \rho/p$. These are a set of non-linear equations in the unknown downstream quantities. However, they can be reduced to one transcendental equation for z_+, which is solved numerically, from which the other downstream quantities can be deduced. The first step in obtaining the equation for z_+ involves the invariance across the shock of na, $V^\alpha V_\alpha$, $W^\alpha V_\alpha$, $W^\alpha l_\alpha - V^\alpha V_\alpha$ and $X^\alpha X_\alpha$ where $X^\alpha = W^\alpha - (a^2nG + n/z + |b|^2/2)l^\alpha$. This leads to five equations for the five unknowns a_+, $|b|^2_+$, d_+, n_+ and z_+. These are

$$[na] = 0 \tag{B26}$$

$$\left[a^2|b|^2 - d^2\right] = 0 \tag{B27}$$

$$[dG] = 0 \tag{B28}$$

$$\left[a^2nG + \frac{n}{z} + \frac{|b|^2}{2}\right] = 0 \tag{B29}$$

$$\left[a^2n^2G^2\left(1 + a^2\right) + \frac{2n}{z}\left(d^2 - a^2|b|^2\right) + 2a^2|b|^2nG\right] = 0 \tag{B30}$$

For algebraic simplicity we introduce the quantities $M \equiv na$, $Q \equiv (a^2|b|^2 - d^2)/M$, $P \equiv dG/\sqrt{M}$ and $D_+ \equiv (Q + P^2/G_+^2)/2$ and the five equations can be written as [10]

$$[M] = [Q] = [P] = 0 \tag{B31}$$

$$a_+G_+ + \frac{1}{a_+z_+} + \frac{D_+}{a_+^2} = c_1 \tag{B32}$$

$$(1 + a_+^2)G_+^2 + \frac{2}{a_+}\left(2D_+G_+ - \frac{Q}{z_+}\right) = c_2 \tag{B33}$$

where c_1 and c_2 are determined by the given upstream state. Equations (B32) and (B33) contain just the two unknowns a_+ and z_+ since D_+ and G_+ are functions of z_+ and all other quantities are given by the upstream parameters. These two jump conditions can be manipulated into a linear equation for a_+

$$a_+ = \frac{\left(c_2 + G_+/z_+ - G_+^2\right)\beta - (\alpha + D_+G_+)\,\alpha c_1}{c_1\beta G_+ - \alpha^2 G_+}. \tag{B34}$$

where

$$\alpha \equiv 3D_+G_+ - \frac{2Q}{z_+} \quad \text{and} \quad \beta \equiv \frac{4D_+G_+}{z_+} - \frac{2Q}{z_+^2} - D_+G_+^2 + D_+c_2.$$

Inserting into either (B32) or (B33) gives a transcendental equation for z_+ which can be solved by a root finding algorithm.

For a dynamically unimportant magnetic field the flow velocities are directed along the shock normal so that Eq.(28) holds. A second relation between upstream and downstream magnetic fields can be obtained from (B27) which becomes

$$\Gamma_-^2 B_-^2 \left(v_-^2 - \cos^2 \Phi_-\right) = \Gamma_+^2 B_+^2 \left(v_+^2 - \cos^2 \Phi_+\right).$$

When combined with Eq.(28) this gives the relationship (Eq.29) between B_+, the upstream parameters and the shock compression ratio which is obtained from the hydrodynamic jump conditions.

Appendix C. The eigenvalues of the relativistic transport equation

In the diffusion approximation, it is assumed that the distribution function is everywhere close to isotropy. Applying this idea to the region far upstream of a shock front suggests that some information about the eigenvalue $\Lambda_{i=1}^v$ and its eigenfunction $Q_{i=1}^v(\mu)$ for small v. may be gained by a perturbative approach. This is indeed the case, and one finds (assuming $D_{\mu\mu}$ is an even function of μ)

$$Q_1^v(\mu) = 1 - \frac{\Lambda_1^v}{2} \int_{-1}^{+1} d\mu' \, \frac{1 - \mu'^2}{D_{\mu'\mu'}}. \tag{C35}$$

and

$$\Lambda_1^v = 8v \left[\int_{-1}^{+1} d\mu \, \frac{\left(1 - \mu^2\right)^2}{D_{\mu\mu}} \right]^{-1}. \tag{C36}$$

This can be expressed in terms of the spatial diffusion coefficient κ, which relates the gradient of the particle density to the flux:

$$\kappa = c^2 / \Lambda_1^v \tag{C37}$$

(where we have explicitly reintroduced the particle speed c) in agreement with the expression given, for example, by Skilling [131]).

In the ultrarelativistic case, particles which cross the shock from downstream to upstream have their pitch angles concentrated in a very narrow cone $-1 < \mu < v_-$, as seen in the upstream rest frame. This indicates that a change of independent variable is appropriate. Choosing $y = (1 + \mu)/(1 - v)$, and approximating $D_{\mu\mu}$ by the first term in its Taylor expansion about $\mu = -1$: $D_{\mu\mu} \approx d(1 + \mu)$ transforms Eq. (44) into

$$yQ'' + Q' + \epsilon^2 \Lambda (y - 1) Q/d = 0 \tag{C38}$$

([62]) where a prime indicates differentiation with respect to y and we have simplified the notation for Q and Λ. We have also introduced the small parameter $\epsilon = 1 - v \approx 1/(2\Gamma^2)$. For large y, the solutions to this equation have the asymptotic dependence $Q \sim \exp(\pm \epsilon y \sqrt{\Lambda/d})$, whereas the regular solution close to the singular point $y = 0$ has the dependence $Q \propto 1 - (\Lambda\epsilon^2/3d)y + \mathrm{O}(y^2)$. Therefore, bounded solutions are of the form

$$Q(y) = \exp(-\epsilon y\sqrt{\Lambda/d}) \sum_{n=0}^{N} a_n y^n, \tag{C39}$$

i.e., a polynomial with an exponential factor. Inserting this into Eq. (C38) and requiring that a_{N+1} vanish yields the positive eigenvalues:

$$\Lambda_i^v \approx d(2i-1)^2/\epsilon^2. \tag{C40}$$

In addition, the following recursion relation is obtained:

$$a_{n+1} = -\frac{2(2N+1)(N-n)}{(n+1)^2}\, a_n. \tag{C41}$$

The eigenfunctions $Q_i^v(\mu)$ are found from these equations by setting $N = i - 1$ and $y = (1+\mu)/(1-v)$.

References

[1] Gaidos J.A. et al. 1996 *Nature* **383**, 318
[2] Metzger, M.R., et al. 1997 *Nature* **387**, 87
[3] Rees M.J. 1966 *Nature* **211**, 468
[4] Vermeulen, R.C., Cohen, M.H. 1994 *Ap. J.* **430**, 467
[5] Taub, A.H. 1948 *Phys. Rev.* **74**, 328
[6] de Hoffmann F., Teller E. 1950 *Phys. Rev.* **80**, 692
[7] Akhiezer I.A., Polovin R.V. 1959 *Sov. Phys. JETP* **9**, 1316
[8] Lichnerowicz A., 1970 *Physica Scripta* **2**,221
[9] Webb G.M., Zank G.P., McKenzie J.F. 1987 *J. Plasma Phys.* **37**, 117
[10] Majorana A., Anile A.M., 1987 *Phys. Fluids* **30**, 3045
[11] Appl S., Camenzind M. 1988 *Astron. Astrophys.* **206**, 258
[12] Kundt W., Krotscheck E., 1982 *Astron. Astrophys.* **83**, 1
[13] Landau, L. D. and Lifshitz, E. M. 1959 *Fluid Mechanics* (London: Pergamon Press).
[14] Blandford, R. D. and McKee, C. F. 1976 *Phys. Fluids* **19**, 1130.
[15] Königl, A. 1980 *Phys. Fluids* **23**, 1083
[16] Akhiezer A.I., Liubarskii G.I., Polovin R.V. 1959 *Sov. Phys. JETP* **8**, 507
[17] Kennel C.F., Edmiston J.P., Hada T. 1983 in 'Collisionless Shocks in the Heliosphere: A Tutorial Review' Eds: B.T. Tsurutani, R.G. Stone, Geophysical Monograph 34, American Geophysical Union, Washington D.C..
[18] van Putten M.H.P.M. 1991 *Commun. Math. Phys.* **141**, 63
[19] van Putten M.H.P.M. 1991 *J. Comp. Phys.* **105**, 339
[20] Falle S.A.E.G., Komissarov S., Joarder P. 1998 *M. N. R. A. S.* **297**, 265
[21] Isenberg P.A., 1986 *J. Geophys. Res.* **91**, 1699
[22] Kirk, J.G., Heavens, A.F. 1989 *M. N. R. A. S.* **239**, 995
[23] Begelman, M.C., Kirk, J.G. 1990 *Ap. J.* **353**, 66

[24] Lichnerowicz A., 1967 'Relativistic Hydrodynamics and Magnetohydrodynamics', (Benjamin, New York) page 172.

[25] Rees M.J., Gunn J.E. 1974 *M. N. R. A. S.* **167**, 1

[26] Kennel C.F., Coroniti F.V., 1984 *Ap. J.* **283**, 694

[27] Michel, F.C. 1991, 'Theory of Neutron Star Magnetospheres', University of Chicago Press, Chicago.

[28] Ballard K.R., Heavens A.F., 1991 *M. N. R. A. S.* **251**, 438

[29] Hall, D.E., Sturrock, P.A. 1967 *Phys. Fluids* **10**, 2620

[30] Melrose, D.B. 1969 *Astrophys.& Space Sci.* **4**, 143

[31] Luhmann, J.G. 1976 *J. Geophys. Res.* **81**, 2089

[32] Achatz, U., Steinacker, J., Schlickeiser, R. 1991 *Astron. Astrophys.* **250**, 266

[33] Lee M.A. 1982 *J. Geophys. Res.* **87**, 5063

[34] Lee M.A. 1983 *J. Geophys. Res.* **88**, 6109

[35] Jokipii J.R., 1966 *Ap. J.* **146**, 480

[36] Hasselmann K., Wibberenz G., 1970 *Ap. J.* **162**, 1049

[37] Parker, E.N. 1965 *Planet. Space Sci.* **13**, 9

[38] Gleeson, L.J., Axford, W.I. 1967 *Ap. J. Letters* **149**, L115

[39] Krymsky, G.F. 1977 *Sov. Phys. Dokl.* **22**, 327

[40] Axford, W.I., Leer, E., Skadron, G. 1977 *Proc. 15th. Int. Cosmic Ray Conf.* (Plodiv) **11**, 132

[41] Bell, A.R. 1978 *M. N. R. A. S.* **182**, 147

[42] Blandford, R.D., Ostriker, J.P. 1978 *Ap. J. Letters* **221**, L29

[43] Drury, L.O'C. 1983 *Rep. Prog. Phys.* **46**, 973

[44] Kirk J.G., Melrose D.B., Priest E.R., 1994 *Plasma Astrophysics*, Saas Fee Advanced Course 24, Eds.: A.O.Benz, T.J.-L. Courvoisier, (Springer-Verlag, Berlin).

[45] Gallant Y.A., Achterberg A., Kirk J.G. 1998 in "Rayos cósmicos 98", Proc. 16th. European Cosmic Ray Symposium, Alcalà Ed. J. Medina, Univ. de Alcalà (Madrid) p. 371

[46] Hoshino M., Arons J., Gallant Y.A., Langdon A.B. 1992 *Ap. J.* **390**, 454

[47] Gallant Y.A., Hoshino M., Langdon A.B., Arons J., Max C.E., 1992 *Ap. J.* **391**, 73

[48] Gallant Y.A., Arons J. 1994 *Ap. J.* **435**, 230

[49] Scheuer P., 1989 in 'Hot-Spots in Extragalactic Radio Sources' Eds. K. Meisenheimer, H.-J. Röser, (Springer-Verlag, Berlin) Lecture Notes in Physics **327**, 159

[50] Parker, E.N. 1958 *Phys. Rev.* **109**, 1328

[51] Schatzman, E. 1963 *Annales d'Astrophys.* **26**, 234

[52] Decker, R.B. 1988 *Space Sc. Rev.* **48**, 195

[53] Whipple, E.C., Northrop, T.G., Birmingham, T.J. 1986 *J. Geophys. Res.* **91**, 4149

[54] Abramowitz, M., Stegun, I.A. 1972 *Handbook of Mathematical Functions* (Washington DC: National Bureau of Standards)

[55] van der Laan, H. 1962 *M. N. R. A. S.* **124**, 125

[56] Gieseler U.D.J., Kirk J.G., Gallant Y.A., Achterberg A. 1999 *Astron. Astrophys.* **345**, 298

[57] Peacock, J.A. 1981 *M. N. R. A. S.* **196**, 135

[58] Kirk J.G., Schneider P. 1987a *Ap. J.* **315**, 425

[59] Ostrowski M., 1991 *M. N. R. A. S.* **249**, 551

[60] Naito T., Takahara F., 1995 *M. N. R. A. S.* **275**, 1077

[61] Schneider P., Kirk J.G., 1989 *Astron. Astrophys.* **217**, 344

[62] Kirk, J.G., Schneider, P. 1989 *Astron. Astrophys.* **225**, 559

[63] Malkov M.A., Völk H.J., 1995 *Astron. Astrophys.* **300**, 605
[64] Kirk, J.G., Schneider, P. 1988 *Astron. Astrophys.* **201**, 177
[65] Baring M.G., Kirk J.G., 1991 *Astron. Astrophys.* **241**, 329
[66] Drury L.O'C., Völk H.J. 1981 *Ap. J.* **248**, 344
[67] Kirk, J.G., Schlickeiser, R., Schneider, P. 1988 *Ap. J.* **328**, 269
[68] Ince E.L., 1956 'Ordinary Differential Equations' (Dover, New York)
[69] Kirk J.G., 1988 Habilitationsschrift, LMU München
[70] Heavens, A.F., Drury, L.O'C. 1988 *M. N. R. A. S.* **235**, 997
[71] Völk, H.J., Morfill, G., Alpers, W., Lee, M.A. 1974 *Astrophys.& Space Sci.* **26**, 403
[72] Bednarz J., Ostrowski M., 1998 *Phys. Rev. Letts.* **80**, 3911
[73] Ballard K.R., Heavens A.F., 1992 *M. N. R. A. S.* **259**, 89
[74] Ostrowski M., 1993 *M. N. R. A. S.* **264**, 248
[75] Rax J.M., White R.B., 1992 *Phys. Rev. Letts.* **68**, 1523
[76] Kirk J.G., Duffy P., Gallant Y.A., 1996 *Astron. Astrophys.* **314**, 1010
[77] Achterberg A., 1988 *M. N. R. A. S.* **232**, 323
[78] Gardiner C.W., 1983 'Handbook of Stochastic Methods' (Springer-Verlag, Berlin)
[79] Kirk, J.G., Schneider, P. 1987b *Ap. J.* **322**, 256
[80] Krülls W., Achterberg A. 1994 *Astron. Astrophys.* **286**, 314
[81] Zachary, A. 1987 *Resonant Alfvén Wave Instabilities Driven by Streaming Fast Particles*, Ph.D. thesis, Lawrence Livermore National Laboratory, University of California.
[82] Jones, F.C., Ellison, D.C. 1991 *Space Sc. Rev.* **58**, 259
[83] Ellison D.C., Jones F.C., Reynolds S.P., 1990 *Ap. J.* **360**, 702
[84] Quenby J.J., Lieu R., 1989 *Nature* **342**, 654
[85] Lieu R., Quenby J.J., Drolias B., Naidu K., 1994 *Ap. J.* **421**, 211
[86] Bednarz J., Ostrowski M., 1996 *M. N. R. A. S.* **283**, 447
[87] Ellison D.C., Baring M.G., Jones F.C., 1996 *Ap. J.* **473**, 1029
[88] Waxman, E. 1997 *Ap. J.* **485**, L5
[89] Galama T.J., Wijers R.A.M.F., Bremer M., Groot P.J., Strom R.G., De Bruyn A.G., Kouveliotou C., Robinson C.R., Van Paradijs J. 1998 *Ap. J. Letters* **500**, L101
[90] Marcowith A., Henri G., Pelletier, G. 1995 *M. N. R. A. S.* **277**, 681
[91] Romanova M.M., Lovelace R.V.E. 1997 *Ap. J.* **475**, 97
[92] Levinson A. 1998 *Ap. J.* **507**, 145
[93] Kirk J.G., Rieger F.M., Mastichiadis A. 1998 *Astron. Astrophys.* **333**, 452
[94] Begelman, M.C., Blandford, R.D., Rees, M.J. 1984 *Rev. Mod. Phys.* **56**, 255
[95] Meisenheimer, K., Heavens, A.F. 1986 *Nature* **323**, 419
[96] Heavens, A.F., Meisenheimer, K. 1987 *M. N. R. A. S.* **225**, 335
[97] Meisenheimer, K., Röser, H.-J., Hiltner, P.R., Yates, M.G., Longair, M.S., Chinis, R., Perley, R.A. 1989 *Astron. Astrophys.* **219**, 63
[98] Wilson, M.J., Scheuer, P.A.G. 1983 *M. N. R. A. S.* **205**, 449
[99] Gomez J.L., Marti J.M., Marscher A.P., Ibañez J.M., Alberdi A. 1997 *Ap. J. Letters* **482**, L33
[100] Mioduszewski A.J., Hughes P.A., Duncan G.C. 1997 *Ap. J.* **476**, 649
[101] Komissarov S., Falle S.A.E.G. 1997 *M. N. R. A. S.* **288**, 833
[102] Matthews, A.P., Scheuer, P.A.G. 1990 *M. N. R. A. S.* **242**, 616
[103] Matthews, A.P., Scheuer, P.A.G. 1990 *M. N. R. A. S.* **242**, 623

[104] Marscher A.P., Gear, W.K. 1985 *Ap. J.* **298**, 114
[105] Hughes P.A., Aller H.D., Aller M.F. 1991 *Ap. J.* **374**, 57
[106] Marscher A.P., Travis J.P., 1996 *Astron. Astrophys. Suppl.* **120C**, 537
[107] Wagner S.J., Witzel A. 1995 *Ann. Rev. Astron. Astrophys.* **33**, 163
[108] Aharonian F., et al. 1999 *Astron. Astrophys.* **342**, 69
[109] Dermer C.D., Schlickeiser R. 1993 *Ap. J.* **416**, 458
[110] Ghisellini G., Maraschi L., Dondi L. 1996 *Astron. Astrophys. Suppl.* **120C**, 503
[111] Stecker F.W., de Jager O.C., Salamon M.H. 1996 *Ap. J. Letters* **473**, L75
[112] Mastichiadis A., Kirk, J.G. 1997 *Astron. Astrophys.* **320**, 19
[113] Mannheim K., Westerhoff S., Meyer H., Fink H.-H. 1996 *Astron. Astrophys.* **315**, 77
[114] Cavallo, G., Rees, M.J. 1978 *M. N. R. A. S.* **183**, 359
[115] Goodman, J. 1986 *Ap. J. Letters* **308**, L47
[116] Paczynski, B. 1986 *Ap. J. Letters* **308**, L43
[117] Rees, M.J., Mészáros, P. 1992 *M. N. R. A. S.* **258**, 41P
[118] Blandford R.D., McKee C.F. 1977 *M. N. R. A. S.* **180**, 343
[119] Mészáros, P., Laguna, P., Rees, M.J. 1993 *Ap. J.* **415**, 181
[120] Piran, T., Shemi, A., Narayan, R. 1993 *M. N. R. A. S.* **263**, 861
[121] Sari, R., Piran, T. 1995 *Ap. J. Letters* **455**, L143
[122] Rees, M.J., Mészáros, P. 1994 *Ap. J. Letters* **430**, L93
[123] Sari, R., Piran, T. 1997 *M. N. R. A. S.* **287**, 110
[124] Vietri, M. 1995 *Ap. J.* **453**, 883
[125] Waxman, E. 1995 *Phys. Rev. Letts.* **75**, 386
[126] Mészáros, P., Rees, M.J. 1993 *Ap. J. Letters* **418**, L59
[127] Dermer, C.D. 1998 *Ap. J. Letters* **501**, 157
[128] Wijers, R.A.M.J., Rees, M.J., Mészáros, P. 1997 *M. N. R. A. S.* **288**, L51
[129] Synge, J. L. 1957 *The Relativistic Gas* (Amsterdam: North-Holland Publishing Co.)
[130] Johnson M.H., McKee C.F. 1971 *Phys. Rev.* **D3**, 858
[131] Skilling, J. 1975 *M. N. R. A. S.* **172**, 557